This article has been accepted for publication in a future issue of this journal, but has not been fully edited. Content may change prior to final publication. Citation information: DOI 10.1109/TVT.2020.2979267, IEEE Transactions on Vehicular Technology

Energy-Aware Relay Selection Improves Security-Reliability Tradeoff in Energy Harvesting Cooperative Cognitive Radio Systems

Peishun Yan, Yulong Zou, *Senior Member, IEEE*, Xiaojin Ding, and Jia Zhu

***Abstract*—This paper investigates the physical layer security for a cooperative cognitive radio (CCR) system with energy-harvesting (EH) technique, which consists of a cognitive source (CS), multiple cognitive relays (CRs) and a cognitive destination (CD) as well as multiple eavesdroppers (Es) who are considered to tap the confidential transmission from CS via CRs to CD. Both CS and CRs are equipped with energy-harvesters to harvest energy from the surrounding radio frequency environment. Additionally, in order to guarantee the quality-of-service of primary communications, the transmit powers of CS and CRs are limited by the maximum tolerant power at primary destination. Depending on the availability of channel state information (CSI) of wireless energy links from primary transmitter (PT) to CRs, we respectively propose non-energy aware relay selection (NEARS) and energy aware relay selection (EARS) schemes for protecting the transmission from CS via CRs to CD from leaking to Es. We consider the use of the security-reliability tradeoff (SRT) to measure the performance of NEARS and EARS schemes. For the purpose of comparison, we also carry out the analysis of SRT performance for conventional direct communication (DC). Furthermore, the closed-form expressions of outage probability and intercept probability for NEARS and EARS schemes are derived and numerical results show that the SRT performance of EARS is better than that of DC and NEARS schemes.**

***Index Terms*—Physical layer security, security-reliability tradeoff, energy harvest, relay selection, cognitive radio.**

I. Introduction

A. Background

With the explosive growth of mobile communications, the wireless devices such as smart phones and unmanned aerial vehicles (UAVs), have penetrated into many aspects of our life, gradually [1]. As we all know, these wireless terminals are powered by the battery with finite capacity. Consequently, the development and deployment of mobile networks have been seriously subject to unsustainable power supply [2]. In recent years, energy-harvesting (EH) technique [2]-[4] has been attracted much attention and considered as a fundamentally promising technology to improve the energy efficiency of wireless devices. The relaying protocols based on EH are divided into time-switching relaying (TSR) protocol and power-splitting relaying (PSR) protocol [5]-[7]. More specifically, the relay first harvests energy from the ambient surroundings within given time and then the harvested energy is used for forwarding source information in TSR protocol. While in PSR protocol, the received power is split into two parts, which are used for information transmission and energy storage. However, the energy efficiency have been enhanced aided with EH technique, the private transmission still faces the serious threaten from vicious attackers due to the broadcast nature of wireless mediums.

B. Related Works

Physical layer security [8] and [9] has been seen as a promising method to prevent the private information from leaking to the eavesdroppers by making use of physical characteristics of wireless links. In [10], Wyner first proposed notion of the secrecy capacity which is the difference between the capacity of main channel (from legitimate source to legitimate destination) and that of wiretap channel (from legitimate source to eavesdropper). Whilst, [10] certified that the intercept event will happen if the secrecy capacity is less than zero. A large number of existing works have paid attention to increasing the secrecy capacity such as cooperative relay selection [11]-[13], multi-input and multi-output (MIMO) [14]-[16] and multiuser scheduling [17] and [18].

In order to improve physical layer security, [12] proposed optimal single relay selection and two-step single relay selection as well as optimal dual relay selection to decrease the secrecy outage probability in a non-orthogonal multiple access system under Nakagami-m channels. While [13] theoretically analyzed the physical layer security in cooperative cognitive radio systems. In [14], MIMO was employed to combat against the eavesdropping attack in a non-cognitive radio system, where optimal antenna selection (OAS) and suboptimal antenna selection (SAS) were proposed to decrease the intercept probability. [15] extended the results of [14] into cognitive radio systems over Nakagami-m fading channels. Moreover, [17] examined the physical layer security in a cognitive radio system which is composed of one common cognitive base station and multiple cognitive users while an eavesdropper may overhear the legitimate transmission. The authors in [18]

This work was partially supported by the National Natural Science Foundation of China (Grant Nos. 61671253, 61631020, and 91738201), and the Natural Science Foundation of Jiangsu Province (Grant No. BK20171446).

P. Yan, Y. Zou and J. Zhu are with the School of Telecommunications and Information Engineering, Nanjing University of Posts and Telecommunications, Nanjing 210003, China. X. Ding is with the Jiangsu Engineering Research Center of Communication and Network Technology, Nanjing University of Posts and Telecommunications, Nanjing 210003, China.

Corresponding authors are Peishun Yan, Yulong Zou, Xiaojin Ding and Jia Zhu. (E-mail: 2019010215@njupt.edu.cn, yulong.zou@njupt.edu.cn, dxj@njupt.edu.cn and jiazhu@njupt.edu.cn).

proposed random jammer selection aided multiuser scheduling and optimal jammer selection aided multiuser scheduling to enhance the secrecy outage performance. Moreover, the numerical results indicated that multiuser scheduling aided with friendly jammer selection outperforms the conventional multiuser scheduling without jammer selection in terms of secrecy outage performance.

Recently, EH combined with physical layer security has became a hot topic [19]-[24]. In [20], the authors studied a PSR system in the view of secrecy transmission. The system outage probability for the linear and nonlinear EH models were derived. Additionally, the analysis of effect of power split ratio and different relay's location as well as different eavesdropper's location on secrecy outage probability were carried out. Differing from [20], the EH untrusted relay was employed to assist the confidential transmission between source and destination for PSR and TSR protocols in [21]. For the purpose of improving the secrecy transmission, [22] and [23] examined the secrecy outage performance jointly aided with relay and jammer selection. The authors in [23] employed best-relay-best-jammer (BRBJ) selection to enhance the secrecy performance for cooperative communications. The results indicated that the secrecy outage performance of BRBJ is superior to BRRJ [22] and RRBJ [22] schemes. The secrecy outage performance for dual-hop mixed radio frequency-free space optical downlink simultaneous wireless information and power transfer system were analyzed in [24]. While [25]-[27] exploited the interference alignment to fight against attacks by eavesdroppers in wireless power transfer systems.

As discussed in [19]-[27], EH non-cognitive radio systems were exploited. While [28]-[32] examined confidential transmission in EH cognitive radio (CR) systems. For example, Lei *et al*. investigated the secrecy outage performance for MIMO-CR systems with EH technology [28]. Depending on the channel state information of wiretap channels is available or unavailable for cognitive users, optimal antenna selection and suboptimal antenna selection schemes were separately employed to improve the cognitive secrecy transmission. In [29], the energy-aware multiuser scheduling was investigated to improve the cognitive secrecy transmission from cognitive users to cognitive common base station. In [30], the optimal relay selection (ORS) with EH was proposed to ameliorate the wireless physical layer security. It was shown that the ORS with EH achieves better performance than ORS without EH in terms of the tradeoff between secrecy outage probability of primary transmission and ergodic rate of cognitive transmission. Additionally, [32] studied the non-convex problem for maximizing the secrecy rate of primary communication. To elaborate, the primary network took use of two-way mechanism and the optimal cognitive user forwarded the primary signals with harvested energy from ambient radio frequency signals. Furthermore, this problem was separated into three tractable problems because of the non-convexity and the two-tiered iterative algorithm was obtained to optimize the secrecy performance for primary users.

C. Motivation and Contributions

To the best of our knowledge, less existing works were devoted to enhancing the physical layer security in cooperative cognitive radio (CCR) systems combining with energy-harvesting (EH) technique. In this context, we explore the secrecy performance for CCR-EH systems in terms of security-reliability tradeoff (SRT), where a cognitive source (CS) communicates with cognitive destination (CD) assisted by multiple cognitive relays (CRs). Meanwhile, multiple eavesdroppers (Es) may tap the legitimate transmission over wiretap channels. The main contributions are descried as follows.

- We present energy-aware relay selection (EARS) and non-energy aware relay selection (NEARS) schemes to protect cognitive transmission between CS and CD from overhearing by multiple Es in a CCR-EH system. The difference between EARS and NEARS is whether or not dependent on channel state information (CSI) of energy channels from PT to CRs. More specifically, the CR maximizing the capacity of main channels spanning from CRs to CD will be selected for forwarding source signals in EARS scheme. Contrarily, the NEARS scheme only relies on the CSI of CRs-CD.
- We provide closed-form expressions of outage probability (OP) and intercept probability (IP) for EARS and NEARS schemes. For comparison, the analysis of classical direct communication (DC) is carried out in terms of OP and IP. It is shown that our proposed EARS scheme achieves the best performance among EARS, NEARS and DC in the perspective view of SRT.
- It needs to be pointed that we analyze physical layer security in a CCR-EH system, while [4] only considered the outage performance for EH cognitive communication. Differing from [19] and [20] which only considered physical layer security in non-cognitive radio systems, we examine the secrecy transmission in cognitive radio systems. Additionally, the authors in [21]-[23] and [28] only studied the secure transmission with EH technique, while the security and reliability of wireless communications are mutually constrained. As a result, this paper discusses the SRT performance to reveal constraint mechanism between reliability and security.

The rest of this paper is organized as follows. We provide the system model for our CCR-EH system and the criteria of relay selection in Section II. Section III presents the closed-form expressions of OP and IP for our proposed EARS scheme and NEARS scheme as well as DC and the SRT performance is analyzed over Rayleigh fading channels. In section IV, the numerical results are shown to validate our theoretical results of EARS, NEARS and DC schemes. Finally, the concluding remarks are drawn in section V.

II. System Model and Problem Formulation

A. System Model

As shown in Fig. 1, we present DC as a bench-marking scheme where CS transmits confidential information to CD directly. Due to the broadcast nature of wireless mediums, Es can tap the private transmission from CS via CRs to

This article has been accepted for publication in a future issue of this journal, but has not been fully edited. Content may change prior to final publication. Citation information: DOI 10.1109/TVT.2020.2979267, IEEE Transactions on Vehicular Technology

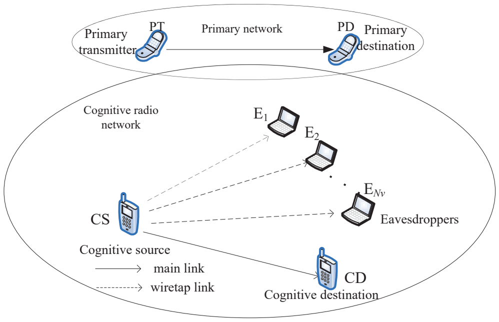

Fig. 1. A Cognitive Radio System with Energy Harvesting technique which consists of a CS, a CD in the face of multiple Es.

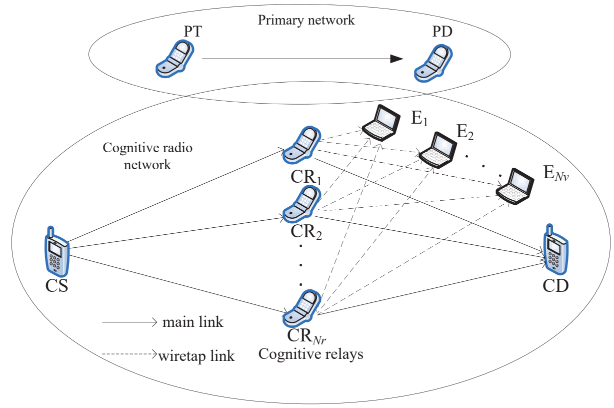

Fig. 2. A Cooperative Cognitive Radio System with Energy Harvesting technique, which is made up of a CS, multiple CRs and a CD in the face of multiple Es.

TABLE I
NOTATIONS AND REPRESENTATIONS

Notations	Representations
AF	Amplify-and-forward
AWGN	Additive white Gaussian noise
CS	Cognitive source
CR	Cognitive relay
CR	Cognitive destination
CDF	Cumulative distribution function
CSI	Channel state information
DC	Direct communication
DF	Decode-and-forward
E	Eavesdropper
EARS	Energy aware relay selection
IP	Intercept probability
MER	Main-to-eavesdropper ratio [8], [14] and [17]
MIMO	multi-input and multi-output
NEARS	Non-energy aware relay selection
OP	Outage probability
PT	Primary transmitter
PR	Primary receiver
SISO	single-input and single-output
SIMO	single-input and multi-output
SRT	Security-reliability tradeoff

CD. We consider a Rayleigh fading model for characterizing all the channels of Fig. 1. We assume that h_{sd}, h_{se}, h_{ps}, h_{sp}, h_{J1} and h_{J2} are the channel gains of CS-CD, CS-E$_e$ $(e = 1, 2, \cdots, N_v)$, PT-CS, CS-PD, PT-CD and PT-E$_e$ respectively. Hence $|h_{sd}|^2$, $|h_{se}|^2$, $|h_{ps}|^2$, $|h_{sp}|^2$, $|h_{J1}|^2$ and $|h_{J2}|^2$ are subject to independently exponential distribution with respective means of σ_{sd}^2, σ_{se}^2, σ_{ps}^2, σ_{sp}^2, σ_{J1}^2 and σ_{J2}^2. Furthermore, this paper considers the case that Es adopt maximum ratio combining [28] and [29] to overhear the confidential information, so even if an E fails to tap the legitimate information, the cognitive secrecy transmission still be threatened by eavesdropping attack. We assume that all nodes in this paper equip single antenna [33]. Following our previous works [29], [34] and other literatures [35], [36] (We have carried out the SRT performance for SIMO [29] and the similar results can be got as SISO [34]. Additionally, the secrecy performance in SIMO [35] was extended into MIMO [36] and the similar performance can be got in terms of secrecy outage probability), the similar SRT results of SISO can be got in MIMO. Moreover, to ensure the quality-of-service of primary transmission, the transmit power of CS shall be limited by the tolerable interference temperature I at PD. The interference at CD and E from PT can be respectively represented as $P_p|h_{J1}|^2$ and $P_p|h_{J2}|^2$. For computational simplicity, we consider that the average interference at CD and an E from PT in the transmitting phase. This can be explained that CD merely pays attention to the signal transmitting channel without focusing on the interfered channel from PT in the transmission phase. Additionally, Fig. 3 in Section IV shows that the performance of average interference from PT is compared with that of instantaneous interference from PT and the performance gap between them does exist. However, the performance gap has no significant effect on our analysis for outage probability and intercept probability. Finally, the thermal noise received at CD and E$_e$ is assumed to be AWGN with zero mean and variance N_0.

B. Direct Communication

The whole communication process is divided into two time slots which are called energy harvesting phase and information transmitting phase. To be specific, CS first harvests energy from PT in αT, where $0 \leq \alpha \leq 1$ is time allocated ratio and T is the time needed to the whole communication. Therefore, the energy harvested at CS in the first phase is given by

$$E_s^{\text{dc}} = \alpha\eta T P_p|h_{ps}|^2, \tag{1}$$

where $0 \leq \eta \leq 1$ and P_p denote the efficiency of energy conversion and the transmit power of PT, respectively. Then, the harvested energy will be utilized to transmit information by CS at the remaining $(1-\alpha)T$. Hence, the transmit power of CS is described as

$$P_s^{\text{dc}} = \min(aP_p|h_{ps}|^2, \frac{I}{|h_{sp}|^2}), \tag{2}$$

where $a = \frac{\alpha\eta}{1-\alpha}$. Upon the theory of Shannon capacity, the capacity of main channel from CS to CD is written as

$$C_d = (1-\alpha)T\log_2(1 + \frac{P_s^{\text{dc}}|h_{sd}|^2}{N_{J1}}), \tag{3}$$

where $N_{J1} = N_0 + P_p\sigma_{J1}^2$. Meanwhile, the confidential information will be intercepted by E$_e$ results from the broadcast

This article has been accepted for publication in a future issue of this journal, but has not been fully edited. Content may change prior to final publication. Citation information: DOI 10.1109/TVT.2020.2979267, IEEE Transactions on Vehicular Technology

and openness nature of wireless communications. Thus, the capacity of wireless channel from CS-E$_e$ is obtained as

$$C_{se} = (1-\alpha)T\log_2(1+\frac{P_s^{\mathrm{dc}}|h_{se}|^2}{N_{J2}}), \tag{4}$$

where $N_{J2} = N_0 + P_p\sigma_{J2}^2$. Here, we consider that Es adopt maximal ratio combining technique to handle the information from CS. As a result, the overall capacity of wiretap channels is given by

$$C_e = (1-\alpha)T\log_2(1+\frac{P_s^{\mathrm{dc}}\sum_{e=1}^{N_v}|h_{se}|^2}{N_{J2}}). \tag{5}$$

C. Non-Energy Aware Relay Selection

Fig. 2 shows that CS transmits confidential information to CD via N_r CRs. Moreover, Es are beyond the coverage of CS due to deep fading and obstacle blocking effects [8] and [13]. Hence, N_v Es who are distributed around CD can overhear the legitimate transmission from CRs. We assume that h_{si}, h_{id}, h_{ie}, h_{pi}, and h_{ip} are the channel gains of CS-CR$_i$ $(i = 1, 2, \cdots, N_r)$, CR$_i$-CD, CR$_i$-E$_e$, PT-CR$_i$ and CR$_i$-PD, respectively. Hence $|h_{si}|^2$, $|h_{id}|^2$, $|h_{ie}|^2$, $|h_{pi}|^2$ and $|h_{ip}|^2$ are subject to independently exponential distribution with respective means of σ_{si}^2, σ_{id}^2, σ_{ie}^2, σ_{pi}^2 and σ_{ip}^2. In addition, the average interference received at CR$_i$ is $E(P_p|h_{Ji}|^2) = P_p\sigma_{Ji}^2$, where h_{Ji} is the CSI of interference channel of PT to CR$_i$. The whole transmission includes three phases. In the first phase αT, CS and CR$_i$ harvest energy from radio frequency signals from PT. The energy collected at CS and CR$_i$ are obtained as

$$E_s = \alpha\eta TP_p|h_{ps}|^2 \tag{6}$$

and

$$E_i = \alpha\eta TP_p|h_{pi}|^2. \tag{7}$$

Therefore, the transmit powers at CS and CR$_i$ are given by

$$P_s = \min(bP_p|h_{ps}|^2, \frac{I}{|h_{sp}|^2}) \tag{8}$$

and

$$P_i = \theta\min(bP_p|h_{pi}|^2, \frac{I}{|h_{ip}|^2}), \tag{9}$$

where $b = \frac{2\alpha\eta}{1-\alpha}$ and θ is the remaining ratio of total harvested energy for transmitting information. Thus, $1-\theta$ is the consumed ratio for decoding, demodulating, re-coding and re-modulating by cognitive relay. The capacity of CS-CR$_i$ can be expressed as

$$C_{si} = \frac{(1-\alpha)T}{2}\log_2(1+\frac{P_s|h_{si}|^2}{N_{Ji}}). \tag{10}$$

where $N_{Ji} = N_0 + P_p\sigma_{Ji}^2$.

In the next phase $\frac{(1-\alpha)T}{2}$, the energy harvested at CS in the αT is employed to transmit cognitive source signal to CRs. In the last remaining time $\frac{(1-\alpha)T}{2}$, CR$_i$ forwards the confidential information from CS to CD. Therefore, the capacity of main link spanning from CR$_i$ to CD can be formulated as

$$C_{id} = \frac{(1-\alpha)T}{2}\log_2(1+\frac{P_i|h_{id}|^2}{N_{J1}}). \tag{11}$$

Additionally, the overall capacity of wireless channels from CR$_i$ to Es is written as

$$C_{ie} = \frac{(1-\alpha)T}{2}\log_2(1+\frac{P_i\sum_{e=1}^{N_v}|h_{ie}|^2}{N_{J2}}). \tag{12}$$

The research findings in [37] indicated that DF protocol has a higher probability of successful decoding and flawless retransmission from a shorter distance than AF protocol if the relay is closer to the source. Moreover, the theoretical results illustrated that the secrecy outage capacity of DF performs better than that of AF at low and medium signal-to-noise ratio (SNR) regimes [38]. Consequently, we assume that all CRs employ DF relaying protocol to deal with the source signal. Specifically, if CR$_i$ fails to decode the received signal, it will not participate in forwarding the source signal. For simplicity, let D to be a set which is composed of CR who can succeed in decoding the signal from CS. By using the law of probability, the sample space of D can be written as

$$\varpi = \{\phi, D_1, D_2, \cdots, D_{2^{N_r}-1}\}, \tag{13}$$

where ϕ means the empty set that all CRs decode received signal unsuccessfully and D_n is the n-th null set. According to the law of Shannon coding, if the channel capacity is lower than the transmission rate R_0, the receiver is incapable of recovering the source signal. Hence, the case $D = \phi$ and $D = D_n$ can be further separately described as

$$D = \phi, \{C_{si} < R_0 | i = 1, 2, 3, \cdots, N_r\} \tag{14}$$

and

$$D = D_n, \left\{C_{si} > R_0, C_{sj} < R_0 | i \in D_n, j \in \overline{D}_n\right\}, \tag{15}$$

where $\overline{D}_n$ denotes the complementary set of D_n. During the last remaining phase $\frac{(1-\alpha)T}{2}$, only one relay is chosen forward information from CS to CD. The selection criterion of NEARS is defined as

$$r = \arg\max_{i\in D_n} |h_{id}|^2, \tag{16}$$

Combining (11) and (16), the capacity of the main channel is rewritten as

$$C_{rd} = \frac{(1-\alpha)T}{2}\log_2(1+\frac{P_r|h_{rd}|^2}{N_{J1}}), \tag{17}$$

where h_{rd} means the wireless channel gain of CR$_r$-CD . Meanwhile, the capacity of wiretap channel is simply formulated as

$$C_{re} = \frac{(1-\alpha)T}{2}\log_2(1+\frac{P_r\sum_{e=1}^{N_v}|h_{re}|^2}{N_{J2}}), \tag{18}$$

where h_{re} denotes the fading coefficient of CR$_r$-E$_e$.

D. Energy Aware Relay Selection

This subsection provides our proposed EARS scheme to enhance physical layer security. The CR_i having the maximal channel capacity of CR_i-CD is considered to be an optimal relay to recover and forward the confidential information. This differs from NEARS which only depends on the CSI of channel spanning from CR_i to CD. Thus, the criterion of EARS is defined as

$$o = \arg\max_{i \in D_n} [\min(b\gamma_{p1}|h_{pi}|^2, \frac{\gamma_{I1}}{|h_{ip}|^2})|h_{id}|^2], \qquad (19)$$

where $\gamma_{p1} = \frac{P_p}{N_{J1}}$, $\gamma_{I1} = \frac{I}{N_{J1}}$. Combining (19) and (11), we can obtain the channel capacity of CR_o-CD

$$C_{od} = \frac{(1-\alpha)T}{2}\log_2(1+\frac{P_o|h_{od}|^2}{N_{J1}}), \qquad (20)$$

where P_o and h_{od} represent the transmit power of CR_o and the fading coefficient of CR_o-CD. Similarly to (18), the channel capacity for Es can be formulated as

$$C_{oe} = \frac{(1-\alpha)T}{2}\log_2(1+\frac{P_o\sum_{e=1}^{N_v}|h_{oe}|^2}{N_{J2}}), \qquad (21)$$

where h_{oe} represents the fading coefficient of channel from CR_o to E_e. As shown in (16) and (19), both the criteria of NEARS and EARS schemes are independent on the CSI of wiretap channel due to the passive eavesdrop by Es. In other words, these two relay selection schemes merely aim to enhance the reliability of cognitive transmission without being beneficial for the wireless capacity of wiretap link.

III. Security and Reliability Analysis Over Rayleigh Fading Channels

In this section, we carry out the analysis of SRT performance for DC, NEARS and EARS schemes over Rayleigh fading channels. As discussed in [39] and [40], the initial message with a secrecy rate R_s is encoded by a secrecy encoder, which generates transmission rate R_0. The difference between R_0 and R_s is extra redundancy to against eavesdropping attacks. We use the OP and IP to respectively evaluate two important metrics: reliability and security. Exactly, the outage event occurs when the capacity of the main channel is lower than transmission data rate R_0, and eavesdropping event happens if the wiretap channel capacity becomes higher than $R_0 - R_s$. Therefore, the OP and IP are separately given by

$$P_{\text{out}} = \Pr(C_d < R_0) \qquad (22)$$

and

$$P_{\text{int}} = \Pr(C_e > R_0 - R_s), \qquad (23)$$

where C_d and C_e denote the capacities received at destination and eavesdropper.

A. Direct Communication

As a baseline, this subsection first analyzes the SRT performance of DC scheme. Using (2), (3) and (22), the OP of DC can be written as

$$\begin{aligned} P_{\text{out}}^{\text{dc}} &= \Pr(C_d < R_0) \\ &= \Pr[\min(a\gamma_{p1}|h_{ps}|^2, \tfrac{\gamma_{I1}}{|h_{sp}|^2})|h_{sd}|^2 < \lambda_0] \end{aligned}, \qquad (24)$$

where $\lambda_0 = 2^{\frac{R_0}{(1-\alpha)T}} - 1$. After some manipulations, $P_{\text{out}}^{\text{dc}}$ can be further rewritten as

$$P_{\text{out}}^{\text{dc}} = P_{\text{out,I}}^{\text{dc}} + P_{\text{out,II}}^{\text{dc}}, \qquad (25)$$

where

$$P_{\text{out,I}}^{\text{dc}} = \Pr(a\gamma_{p1}|h_{ps}|^2|h_{sd}|^2 < \lambda_0, a\gamma_{p1}|h_{ps}|^2 < \frac{\gamma_{I1}}{|h_{sp}|^2}) \qquad (26)$$

and

$$P_{\text{out,II}}^{\text{dc}} = \Pr(\frac{\gamma_{I1}}{|h_{sp}|^2}|h_{sd}|^2 < \lambda_0, a\gamma_{p1}|h_{ps}|^2 > \frac{\gamma_{I1}}{|h_{sp}|^2}). \qquad (27)$$

Using the results of Appendix A, the closed-form expressions of $P_{\text{out,I}}^{\text{dc}}$ and $P_{\text{out,II}}^{\text{dc}}$ can be respectively expressed as

$$\begin{aligned} P_{\text{out,I}}^{\text{dc}} = 1 &- \sqrt{\frac{\varepsilon_1\gamma_{I1}}{\sigma_{sp}^2}}K_1(\sqrt{\frac{\varepsilon_1\gamma_{I1}}{\sigma_{sp}^2}}) - \sqrt{\frac{\varepsilon_1\lambda_0}{\sigma_{sd}^2}} \\ &\times K_1(\sqrt{\frac{\varepsilon_1\lambda_0}{\sigma_{sd}^2}}) + \sqrt{\varepsilon_1\varepsilon_2}K_1(\sqrt{\varepsilon_1\varepsilon_2}) \end{aligned} \qquad (28)$$

and

$$P_{\text{out,II}}^{\text{dc}} = \sqrt{\frac{\varepsilon_1\gamma_{I1}}{\sigma_{sp}^2}}K_1(\sqrt{\frac{\varepsilon_1\gamma_{I1}}{\sigma_{sp}^2}}) - \frac{\gamma_{I1}}{\sigma_{sp}^2}\sqrt{\frac{\varepsilon_1}{\varepsilon_2}}K_1(\sqrt{\varepsilon_1\varepsilon_2}), \qquad (29)$$

where $K_n(x)$ represents modified bessel function of order n [41]. Therefore, substituting (28) and (29) into (25), $P_{\text{out}}^{\text{dc}}$ can be rewritten as

$$\begin{aligned} P_{\text{out}}^{\text{dc}} = 1 &- \sqrt{\tfrac{\varepsilon_1\lambda_0}{\sigma_{sd}^2}}K_1(\sqrt{\tfrac{\varepsilon_1\lambda_0}{\sigma_{sd}^2}}) - \tfrac{\gamma_{I1}}{\sigma_{sp}^2} \\ &\times \sqrt{\tfrac{\varepsilon_1}{\varepsilon_2}}K_1(\sqrt{\varepsilon_1\varepsilon_2}) + \sqrt{\varepsilon_1\varepsilon_2}K_1(\sqrt{\varepsilon_1\varepsilon_2}) \end{aligned}. \qquad (30)$$

Additionally, combining (5) with (23), we can obtain the corresponding IP of DC scheme as

$$\begin{aligned} P_{\text{int}}^{\text{dc}} &= \Pr(C_e > R_0 - R_s) \\ &= \Pr[\min(a\gamma_{p2}|h_{ps}|^2, \tfrac{\gamma_{I2}}{|h_{sp}|^2})\sum_{e=1}^{N_v}|h_{se}|^2 > \lambda_s] \end{aligned}. \qquad (31)$$

where $\lambda_s = 2^{\frac{R_0-R_s}{(1-\alpha)T}} - 1$, $\gamma_{p2} = \frac{P_p}{N_{J2}}$ and $\gamma_{I2} = \frac{I}{N_{J2}}$. After some mathematical manipulations, $P_{\text{int}}^{\text{dc}}$ is reformulated as

$$P_{\text{int}}^{\text{dc}} = P_{\text{int,I}}^{\text{dc}} + P_{\text{int,II}}^{\text{dc}}, \qquad (32)$$

wherein,

$$P_{\text{int,I}}^{\text{dc}} = \Pr(\sum_{e=1}^{N_v}|h_{se}|^2 > \frac{\lambda_s}{a\gamma_{p2}|h_{ps}|^2}, |h_{sp}|^2 < \frac{\gamma_{I2}}{a\gamma_{p2}|h_{ps}|^2}) \qquad (33)$$

and

$$P_{\text{int,II}}^{\text{dc}} = \Pr(\sum_{e=1}^{N_v}|h_{se}|^2 > \frac{\lambda_s}{\gamma_{I2}}|h_{sp}|^2, |h_{ps}|^2 > \frac{\gamma_{I2}}{a\gamma_{p2}|h_{sp}|^2}). \qquad (34)$$

Referring to the results of Appendix B, we get $P_{\text{int,I}}^{\text{dc}}$ and $P_{\text{int,II}}^{\text{dc}}$ as

$$\begin{aligned} P_{\text{int,I}}^{\text{dc}} = &\sum_{g=0}^{N_v-1} \frac{2{\Lambda_1}^g}{g!\sigma_{ps}^2}(\Lambda_1\sigma_{ps}^2)^{\frac{1-g}{2}} K_{1-g}(2\sqrt{\frac{\Lambda_1}{\sigma_{ps}^2}}) \\ &- \sum_{g=0}^{N_v-1} \frac{2{\Lambda_1}^g}{g!\sigma_{ps}^2}[(\Lambda_1+\Lambda_2)\sigma_{ps}^2]^{\frac{1-g}{2}} K_{1-g}(2\sqrt{(\frac{\Lambda_1+\Lambda_2}{\sigma_{ps}^2}})\end{aligned} \tag{35}$$

and

$$P_{\text{int,II}}^{\text{dc}} = \sum_{g=0}^{N_v-1} \frac{2{\Lambda_3}^g}{g!\sigma_{sp}^2}(\frac{\Lambda_4}{\Lambda_3+\frac{1}{\sigma_{sp}^2}})^{\frac{g+1}{2}} K_{1+g}(2\sqrt{\Lambda_4\Lambda_3+\frac{\Lambda_4}{\sigma_{sp}^2}}). \tag{36}$$

Thus, we can obtain the closed-form expression of $P_{\text{int}}^{\text{dc}}$ by substituting (35) and (36) into (32), which can be further computed as

$$\begin{aligned} P_{\text{int}}^{\text{dc}} = &\sum_{g=0}^{N_v-1} \frac{2{\Lambda_1}^g}{g!\sigma_{ps}^2}(\Lambda_1\sigma_{ps}^2)^{\frac{1-g}{2}} K_{1-g}(2\sqrt{\frac{\Lambda_1}{\sigma_{ps}^2}}) \\ &- \sum_{g=0}^{N_v-1} \frac{2{\Lambda_1}^g}{g!\sigma_{ps}^2}[(\Lambda_1+\Lambda_2)\sigma_{ps}^2]^{\frac{1-g}{2}} K_{1-g}(2\sqrt{\frac{\Lambda_1+\Lambda_2}{\sigma_{ps}^2}}) \\ &+ \sum_{g=0}^{N_v-1} \frac{2{\Lambda_3}^g}{g!\sigma_{sp}^2}[\Lambda_4(\Lambda_3+\frac{1}{\sigma_{sp}^2})^{-1}]^{\frac{g+1}{2}} K_{1+g}(2\sqrt{\Lambda_4(\Lambda_3+\frac{1}{\sigma_{sp}^2})}) \end{aligned} . \tag{37}$$

B. Non-Energy Aware Relay Selection

In this subsection, we consider NEARS scheme to against eavesdropping attacks from the perspective view of physical layer security, where only the CR maximizing $|h_{id}|^2$ is selected to decode and forward source signal in the corresponding time slot. The OP of NEARS is given by

$$P_{\text{out}}^{\text{NEARS}} = \Pr\left(C_{rd} < \gamma_0, D = \phi\right) + \Pr\left(C_{rd} < \gamma_0, D = D_n\right), \tag{38}$$

where $\gamma_0 = 2^{\frac{2R_0}{(1-\alpha)T}} - 1$ and C_{rd} is written as (17). In the case of $D = \phi$, there is no CR being selected to retransmit information from CS to CD. This means that $C_{rd} = 0$. Hence, we can write (38) as

$$P_{\text{out}}^{\text{NEARS}} = \Pr\left(D = \phi\right) + \Pr\left(C_{rd} < \gamma_0, D = D_n\right). \tag{39}$$

Relying on (14), (15) and (17), (39) can be further simplified as

$$P_{\text{out}}^{\text{NEARS}} = \prod_{i=1}^{N_r} \psi_{\text{I}} + \sum_{n=1}^{2^{N_r}-1} \prod_{i\in D_n} (1-\psi_{\text{I}}) \prod_{j\in \overline{D}_n} \psi_{\text{II}} P_{\text{out,I}}^{\text{NEARS}}, \tag{40}$$

wherein, the expressions of ψ_{I}, ψ_{II} and $P_{\text{out,I}}^{\text{NEARS}}$ can be written as

$$\psi_{\text{I}} = \Pr[\min(b\gamma_{pi}|h_{ps}|^2, \frac{\gamma_{Ii}}{|h_{sp}|^2})|h_{si}|^2 < \gamma_0], \tag{41}$$

$$\psi_{\text{II}} = \Pr[\min(b\gamma_{pj}|h_{ps}|^2, \frac{\gamma_{Ij}}{|h_{sp}|^2})|h_{sj}|^2 < \gamma_0] \tag{42}$$

and

$$P_{\text{out,I}}^{\text{NEARS}} = \Pr[\min(b\gamma_{p1}|h_{pr}|^2, \frac{\gamma_{I1}}{|h_{rp}|^2})|h_{rd}|^2 < \lambda_1], \tag{43}$$

where $\lambda_1 = \frac{\gamma_0}{\theta}$, $\gamma_{pi} = \frac{P_p}{N_{Ji}}$, $\gamma_{Ii} = \frac{I}{N_{Ji}}$, $\gamma_{pj} = \frac{P_p}{N_0+P_p\sigma_{Jj}^2}$ and $\gamma_{Ij} = \frac{I}{N_0+P_p\sigma_{Jj}^2}$. Carefully observing from (41) and (42) as well as (24), we can readily reformulate (41) and (42), respectively. Additionally, by using the law of total probability, we arrive at

$$P_{\text{out,I}}^{\text{NEARS}} = \sum_{i\in D_n} \left(P_{\text{out,I\_1}}^{\text{NEARS}} + P_{\text{out,I\_2}}^{\text{NEARS}}\right), \tag{44}$$

wherein, $P_{\text{out,I\_1}}^{\text{NEARS}}$ and $P_{\text{out,I\_2}}^{\text{NEARS}}$ are separately expressed as (45) and (46)

$$\begin{aligned} P_{\text{out,I\_1}}^{\text{NEARS}} = \Pr(&b\gamma_{p1}|h_{pi}|^2|h_{id}|^2 < \lambda_1, b\gamma_{p1}|h_{pi}|^2 \\ &< \tfrac{\gamma_{I1}}{|h_{ip}|^2}, \max_{k\in D_n, k\neq i}|h_{kd}|^2 < |h_{id}|^2) \end{aligned} \tag{45}$$

and

$$\begin{aligned} P_{\text{out,I\_2}}^{\text{NEARS}} = \Pr(&\tfrac{\gamma_{I1}|h_{id}|^2}{|h_{ip}|^2} < \lambda_1, b\gamma_{p1}|h_{pi}|^2 \\ &> \tfrac{\gamma_{I1}}{|h_{ip}|^2}, \max_{k\in D_n, k\neq i}|h_{kd}|^2 < |h_{id}|^2) \end{aligned} . \tag{46}$$

Referring to the results of Appendix C, the final expressions of (45) and (46) can be derived as (47) and (48) at the next page.

Using (14), (15), (18) and (23), the IP of NEARS scheme can be expressed as

$$P_{\text{int}}^{\text{NEARS}} = \Pr\left(C_{re} > \gamma_s, D = \phi\right) + \Pr\left(C_{re} > \gamma_{th}, D = D_n\right), \tag{49}$$

where $\gamma_s = 2^{\frac{2(R_0-R_s)}{(1-\alpha)T}} - 1$. Similarly to (39), if $D = \phi$, all relays fail to recover and forward the source signal, which causes $C_{re} = 0$. As a result, we can reformulate $P_{\text{int}}^{\text{NEARS}}$ as

$$P_{\text{int}}^{\text{NEARS}} = \sum_{n=1}^{2^{N_r}-1} \prod_{i\in D_n} (1-\psi_{\text{I}}) \prod_{j\in \overline{D}_n} \psi_{\text{II}} P_{\text{int,I}}^{\text{NEARS}}, \tag{50}$$

wherein, $P_{\text{int,I}}^{\text{NEARS}}$ can be given by

$$\begin{aligned} P_{\text{int,I}}^{\text{NEARS}} = &\sum_{i\in D_n} \underbrace{\Pr[\min(b\gamma_{p2}|h_{pi}|^2, \frac{\gamma_{I2}}{|h_{ip}|^2}) \sum_{e=1}^{N_v} |h_{ie}|^2 > \lambda_2]}_{P_{\text{int,I\_1}}^{\text{NEARS}}} \\ &\times \underbrace{\Pr(\max_{k\in D_n, k\neq i} |h_{kd}|^2 < |h_{id}|^2)}_{P_{\text{int,I\_2}}^{\text{NEARS}}}. \end{aligned} \tag{51}$$

where $\lambda_2 = \frac{\gamma_s}{\theta}$. It is clearly for us to see that $P_{\text{int,I\_1}}^{\text{NEARS}}$ can be got by substituting b, σ_{pi}^2, σ_{ip}^2, σ_{ie}^2 and λ_2 into (31) by replacing a, σ_{ps}^2, σ_{sp}^2, σ_{se}^2 and λ_s, respectively. In addition, considering $X = |h_{id}|^2$ to be a random variable followed exponential distribution with mean σ_{id}^2. $P_{\text{int,I\_2}}^{\text{NEARS}}$ can be computed as

$$P_{\text{int,I\_2}}^{\text{NEARS}} = \int_0^\infty \prod_{k\in D_n, k\neq i} [1 - \exp(-\frac{x}{\sigma_{kd}^2})] f_X(x)dx, \tag{52}$$

where $f_X(x)$ is the PDF of X, which can be described as $f_X(x) = \frac{1}{\sigma_{id}^2}\exp(-\frac{x}{\sigma_{id}^2})$. Moreover,

$$\begin{aligned} P_{\text{out,I\_1}}^{\text{NEARS}} = & 1-\sqrt{\Lambda_5\lambda_1}K_1(\sqrt{\Lambda_5\lambda_1})-\sqrt{\frac{\gamma_{I1}\Lambda_7}{\sigma_{ip}^2}}K_1(\sqrt{\frac{\gamma_{I1}\Lambda_7}{\sigma_{ip}^2}})+\sqrt{\Lambda_7(\gamma_{I1}\sigma_{ip}^{-2}+\lambda_1\sigma_{id}^{-2})}K_1(\sqrt{\Lambda_7(\gamma_{I1}\sigma_{ip}^{-2}+\lambda_1\sigma_{id}^{-2})}) \\ & +\sum_{m=1}^{2^{|D_n|-1}-1}\frac{(-1)^{|D_n(m)|}\Lambda_6}{\sigma_{id}^2}[1-\sqrt{4\lambda_1\big/(b\gamma_{p1}\Lambda_6\sigma_{pi}^2)}K_1(\sqrt{4\lambda_1\big/(b\gamma_{p1}\Lambda_6\sigma_{pi}^2)})] \\ & -\sum_{m=1}^{2^{|D_n|-1}-1}\frac{(-1)^{|D_n(m)|}\Lambda_6}{\sigma_{id}^2}\sqrt{\gamma_{I1}\Lambda_5}K_1(\sqrt{\gamma_{I1}\Lambda_5})+\sum_{m=1}^{2^{|D_n|-1}-1}\frac{(-1)^{|D_n(m)|}\Lambda_6}{\sigma_{id}^2}\sqrt{\Lambda_8}K_1(\sqrt{\Lambda_8}) \end{aligned} . \quad (47)$$

$$\begin{aligned} P_{\text{out,I\_2}}^{\text{NEARS}} = & \sqrt{\frac{\gamma_{I1}\Lambda_7}{\sigma_{ip}^2}}K_1(\sqrt{\frac{\gamma_{I1}\Lambda_7}{\sigma_{ip}^2}})-\sigma_{ip}^{-2}\sqrt{\frac{\gamma_{I1}\Lambda_7}{\Lambda_9}}K_1(\sqrt{\gamma_{I1}\Lambda_7\Lambda_9})+\sum_{m=1}^{2^{|D_n|-1}-1}\frac{(-1)^{|D_n(m)|}\Lambda_6}{\sigma_{id}^2}\sqrt{\gamma_{I1}\Lambda_7}K_1(\sqrt{\gamma_{I1}\Lambda_7}) \\ & -\sum_{m=1}^{2^{|D_n|-1}-1}\frac{(-1)^{|D_n(m)|}\Lambda_6}{\sigma_{ip}^2\sigma_{id}^2}\sqrt{\frac{\gamma_{I1}\Lambda_7}{\sigma_{ip}^2}+\frac{\lambda_1\Lambda_7}{\Lambda_6}}K_1(\sqrt{\frac{\gamma_{I1}\Lambda_7}{\sigma_{ip}^2}+\frac{\lambda_1\Lambda_7}{\Lambda_6}}) \end{aligned} . \quad (48)$$

$\prod_{k\in D_n,k\neq i}[1-\exp(-\frac{x}{\sigma_{kd}^2})]$ can be expanded by using the binomial theorem

$$\begin{aligned} & \prod_{k\in D_n,k\neq i}[1-\exp(-\frac{x}{\sigma_{kd}^2})] \\ & =1+\sum_{m=1}^{2^{|D_n|-1}-1}(-1)^{|D_n(m)|}\exp(-\sum_{k\in D_n(m)}\frac{x}{\sigma_{kd}^2}) \end{aligned} , \quad (53)$$

where $D_n(m)$ is the m-th non-empty subset of D_n. Therefore, we have

$$\begin{aligned} & P_{\text{int,I\_2}}^{\text{NEARS}} \\ & =\int_0^\infty[1+\sum_{m=1}^{2^{|D_n|-1}-1}(-1)^{|D_n(m)|}\exp(-\sum_{k\in D_n(m)}\frac{x}{\sigma_{kd}^2})]f_X(x)dx \\ & =1+\sum_{m=1}^{2^{|D_n|-1}-1}\frac{(-1)^{|D_n(m)|}}{\sigma_{id}^2}(\sum_{k\in D_n(m)}\frac{1}{\sigma_{kd}^2}+\frac{1}{\sigma_{id}^2})^{-1} \end{aligned} . \quad (54)$$

Hence, substituting ψ_{I}, ψ_{II} and $P_{\text{int,I}}^{\text{NEARS}}$ into (50), $P_{\text{int}}^{\text{NEARS}}$ can be finally obtained.

C. Energy Aware Relay Selection

This subsection presents our proposed EARS scheme to improve the cognitive secrecy transmission in terms of SRT performance. Using (14), (15), (20) and (22), the OP of EARS is written as

$$P_{\text{out}}^{\text{EARS}}=\Pr\left(C_{od}<\gamma_0,D=\phi\right)+\Pr\left(C_{od}<\gamma_0,D=D_n\right), \quad (55)$$

which is similar to (38) and can be further obtained as

$$P_{\text{out}}^{\text{EARS}}=\prod_{i=1}^{N_r}\psi_{\text{I}}+\sum_{n=1}^{2^{N_r}-1}\prod_{i\in D_n}(1-\psi_{\text{I}})\prod_{j\in\overline{D_n}}\psi_{\text{II}}P_{\text{out,I}}^{\text{EARS}}, \quad (56)$$

where ψ_{I} and ψ_{II} are derived as (41) and (42). Additionally, $P_{\text{out,I}}^{\text{EARS}}$ can be expressed as

$$\begin{aligned} P_{\text{out,I}}^{\text{EARS}} & =\Pr(\max_{i\in D_n}\frac{P_i|h_{id}|^2}{N_0}<\gamma_0) \\ & =\prod_{i\in D_n}\Pr[\min(b\gamma_{p1}|h_{pi}|^2,\frac{\gamma_{I1}}{|h_{ip}|^2})|h_{id}|^2<\lambda_1] \end{aligned} . \quad (57)$$

Thus, according to the derivation of ψ_{I}, we can readily get (57). Moreover, the closed-form expression of $P_{\text{out}}^{\text{EARS}}$ can be readily got. We then carry out the analysis of IP for EARS scheme. Similarly to (50), the IP of EARS scheme can be expressed as

$$P_{\text{int}}^{\text{EARS}}=\sum_{n=1}^{2^{N_r}-1}\prod_{i\in D_n}(1-\psi_{\text{I}})\prod_{j\in\overline{D_n}}\psi_{\text{II}}P_{\text{int,I}}^{\text{EARS}}, \quad (58)$$

where

$$P_{\text{int,I}}^{\text{EARS}}=\Pr(\frac{P_o\sum_{e=1}^{N_v}|h_{oe}|^2}{N_{J2}}>\gamma_s). \quad (59)$$

Relying on the theory of total probability, we can further write $P_{\text{int,I}}^{\text{EARS}}$ as

$$P_{\text{int,I}}^{\text{EARS}}=\sum_{i\in D_n}(P_{\text{int,I\_1}}^{\text{EARS}}+P_{\text{int,I\_2}}^{\text{EARS}}), \quad (60)$$

which is composed of $P_{\text{int,I\_1}}^{\text{EARS}}$ and $P_{\text{int,I\_2}}^{\text{EARS}}$ and they are respectively reformulated as

$$\begin{aligned} P_{\text{int,I\_1}}^{\text{EARS}}=\Pr(& \max_{k\in D_n,k\neq i}\tfrac{P_k|h_{kd}|^2}{N_{J2}}<b\gamma_{p2}|h_{pi}|^2|h_{id}|^2, \\ & \sum_{e=1}^{N_v}|h_{ie}|^2>\tfrac{\lambda_2}{b\gamma_{p2}|h_{pi}|^2},|h_{ip}|^2<\tfrac{\gamma_{I2}}{b\gamma_{p2}|h_{pi}|^2},) \end{aligned} \quad (61)$$

and

$$\begin{aligned} P_{\text{int,I\_2}}^{\text{EARS}}=\Pr(& \max_{k\in D_n,k\neq i}\tfrac{P_k|h_{kd}|^2}{N_{J2}}<\tfrac{\gamma_{I2}}{|h_{ip}|^2}|h_{id}|^2, \\ & \sum_{e=1}^{N_v}|h_{ie}|^2>\tfrac{\lambda_2}{\gamma_{I2}}|h_{ip}|^2,|h_{pi}|^2>\tfrac{\gamma_{I2}}{b\gamma_{p2}|h_{ip}|^2}) \end{aligned} . \quad (62)$$

In (61) and (62), $\frac{P_k}{N_{J2}}=\theta\min(b\gamma_{p2}|h_{pk}|^2,\frac{\gamma_{I2}}{|h_{kp}|^2})$. For notational convenience, let X_k and Y_i respectively denote $\frac{P_k}{N_{J2}}|h_{kd}|^2$ and $\sum_{e=1}^{N_v}|h_{ie}|^2$. And the CDF of X_k and Y_i can be respectively computed [28] as

$$\begin{aligned} & F_{X_k}(x_k)=1-\sqrt{\Delta_1\theta^{-1}\sigma_{kd}^{-2}x_k}K_1(\sqrt{\Delta_1\theta^{-1}\sigma_{kd}^{-2}x_k}) \\ & +\sqrt{\Delta_1\Delta_2}K_1(\sqrt{\Delta_1\Delta_2})-\gamma_{I2}\sigma_{kp}^{-2}\sqrt{\Delta_1\Delta_2^{-1}}K_1(\sqrt{\Delta_1\Delta_2}) \end{aligned} \quad (63)$$

and

$$F_{Y_i}(y_i)=1-\exp(-\frac{y_i}{\sigma_{ie}^2})\sum_{g=0}^{N_v-1}\frac{1}{g!}(\frac{y_i}{\sigma_{ie}^2})^g, \quad (64)$$

This article has been accepted for publication in a future issue of this journal, but has not been fully edited. Content may change prior to final publication. Citation information: DOI 10.1109/TVT.2020.2979267, IEEE Transactions on Vehicular Technology

where $\Delta_1 = \frac{4}{b\gamma_{p2}\sigma_{pk}^2}$ and $\Delta_2 = \frac{x_k}{\sigma_{kd}^2} + \frac{\gamma_{I2}}{\sigma_{kp}^2}$. Aided with (63) and (64), we then separately rewrite (61) and (62) as

$$\begin{aligned} P_{\text{int,I\_1}}^{\text{EARS}} = & \iint\limits_{\Xi} \exp(-\frac{\Delta_3}{x}) \sum_{g=0}^{N_v-1} \frac{\Delta_3^g}{g! x^g} (1-\exp(-\frac{\Delta_4}{x})) \\ & \times \prod_{k\in D_n, k\neq i} \Theta(x,y) f_{|h_{pi}|^2}(x) f_{|h_{id}|^2}(y) dxdy \end{aligned} \tag{65}$$

and

$$\begin{aligned} P_{\text{int,I\_2}}^{\text{EARS}} = & \iint\limits_{\zeta} \exp(-\Delta_5 z) \sum_{g=0}^{N_v-1} \frac{\Delta_5^g z^g}{g!} \exp(-\frac{\Delta_6}{z}) \\ & \times \prod_{k\in D_n, k\neq i} \mathrm{T}(y,z) f_{|h_{id}|^2}(y) f_{|h_{ip}|^2}(z) dydz \end{aligned} , \tag{66}$$

where $\Delta_3 = \frac{\lambda_2}{b\gamma_{p2}\sigma_{ie}^2}$, $\Delta_4 = \frac{\gamma_{I2}}{b\gamma_{p2}\sigma_{ip}^2}$, $\Delta_5 = \frac{\lambda_2}{\gamma_{I2}\sigma_{ie}^2}$, $\Delta_6 = \frac{\gamma_{I2}}{b\gamma_{p2}\sigma_{pi}^2}$, Ξ={$(x,y)|x>0, y>0$} and ζ={$(y,z)|y>0, z>0$}. Additionally, with the help of $F_{X_k}(x_k)$, $\Theta(x,y)$ and $\mathrm{T}(y,z)$ can be computed as

$$\begin{aligned} \Theta(x,y) = & 1 - \sqrt{a\gamma_{p2}\Delta_1\theta^{-1}\sigma_{kd}^{-2}xy} K_1(\sqrt{a\gamma_{p2}\Delta_1\theta^{-1}\sigma_{kd}^{-2}}) \\ & + \sqrt{\Delta_1\Delta_2} K_1(\sqrt{\Delta_1\Delta_2}) - \gamma_{I2}\sigma_{kp}^{-2}\sqrt{\Delta_1\Delta_2^{-1}} K_1(\sqrt{\Delta_1\Delta_2}) \end{aligned} \tag{67}$$

and

$$\begin{aligned} \mathrm{T}(y,z) = & 1 - \sqrt{\Delta_1\theta^{-1}\frac{\gamma_{I2}y}{z\sigma_{kd}^2}} K_1(\sqrt{\Delta_1\theta^{-1}\frac{\gamma_{I2}y}{z\sigma_{kd}^2}}) \\ & + \sqrt{\Delta_1\Delta_2} K_1(\sqrt{\Delta_1\Delta_2}) - \gamma_{I2}\sigma_{kp}^{-2}\sqrt{\Delta_1\Delta_2^{-1}} K_1(\sqrt{\Delta_1\Delta_2}) \end{aligned} . \tag{68}$$

It is challenging to get the closed-form expressions of $P_{\text{int,I\_1}}^{\text{EARS}}$ and $P_{\text{int,I\_2}}^{\text{EARS}}$ with our existing knowledge. However, the optimal CR merely relies on the CSI of energy harvesting channels from PT to CRs and main channels from CRs to CD. This results in that only the outage probability of legitimate transmission significantly decreases without enhancing the secrecy transmission obviously. As mentioned above, the PDFs of random variables of $\sum_{e=1}^{N_v} |h_{oe}|^2$, $|h_{op}|^2$ and $|h_{po}|^2$ are the same as $\sum_{e=1}^{N_v} |h_{ie}|^2$, $|h_{ip}|^2$ and $|h_{pi}|^2$. Hence, formula (60) can be reformulated as

$$\begin{aligned} P_{\text{int}}^{\text{EARS}} = & \sum_{m=0}^{N_v-1} \frac{2\Delta_3^m}{m!\sigma_{pi}^2} (\Delta_3\sigma_{pi}^2)^{\frac{1-m}{2}} K_{1-m}(2\sqrt{\Delta_3\sigma_{pi}^{-2}}) \\ & - \sum_{m=0}^{N_v-1} \frac{2\Delta_3^m}{m!\sigma_{pi}^2} [(\Delta_3+\Delta_7\sigma_{ie}^{-2})\sigma_{pi}^2]^{\frac{1-m}{2}} K_{1-m}(2\sqrt{\frac{\Delta_3+\Delta_7\sigma_{ie}^{-2}}{\sigma_{pi}^2}}), \\ & + \sum_{m=0}^{N_v-1} \frac{2\Delta_5^m}{m!\sigma_{ip}^2} [(\Delta_5+\sigma_{ip}^{-2})\Delta_7\sigma_{pi}^2]^{\frac{1+m}{2}} K_{1+m}(2\sqrt{\frac{(\Delta_5+\sigma_{ip}^{-2})\Delta_7}{\sigma_{pi}^2}}) \end{aligned} \tag{69}$$

where $\Delta_7 = \frac{\gamma_{I2}}{a\gamma_{p2}}$.

IV. Numerical Results and Discussions

This section shows the numerical results and discussions about the analysis of DC, NEARS and EARS schemes. The correctness of theoretical OPs and IPs for DC, NEARS and our proposed EARS schemes are verified by Monte-Carlo simulations. Let us denote $\gamma_I = I/N_0$ and $\gamma_p = P_p/N_0$. N_{st}, N_{rt}, N_{dt} and N_{et} respectively represent the antenna numbers at CS, CR, CD and E. For simplicity, let "T" represent the theoretical result, "S" represent the simulated result.

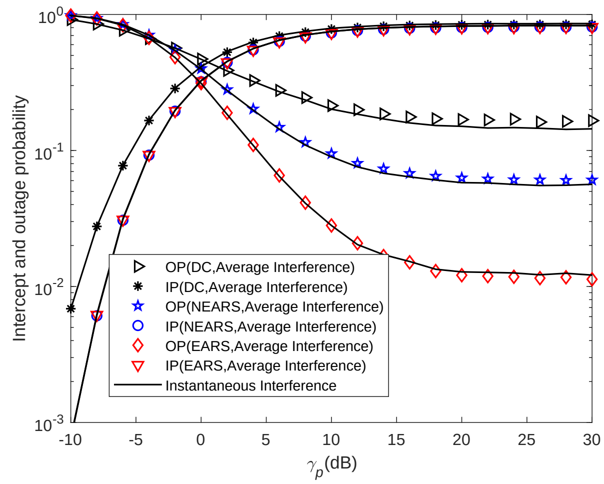

Fig. 3. IPs and OPs of DC and NEARS as well as EARS schemes versus SNR with $\alpha = 0.4$, $\eta = 0.6$, $\theta = 0.8$, $\gamma_I = 20$dB, $\sigma_{sd}^2 = \sigma_{si}^2 = \sigma_{id}^2 = 0.5$, $\sigma_{ps}^2 = \sigma_{pi}^2 = 0.2$, $\sigma_{J1}^2 = \sigma_{J2}^2 = \sigma_{Ji}^2 = 0.2$, $\sigma_{ip}^2 = \sigma_{sp}^2 = 0.2$, MER=10dB, $T = 1$s, $N_r = 4$, $N_v = 4$.

Fig. 3 shows that OPs and IPs versus γ_p for EARS and NEARS as well as DC schemes. One can clearly see that the performance gap of solid lines and discrete dots does exist but it has no obvious impact on our analysis, which indicates that the feasibility of our consideration for average interference at cognitive users from PT. In Fig. 4, the theoretical results match well with our simulated results, certifying the correctness of theoretical OP and IP. Moreover, the performance of OP for EARS is better than that of NEARS and DC. Whilst, the OP performance of these three schemes increases and IP performance decreases with an increasing γ_p. It is shown that a tradeoff exists between security and reliability for cognitive transmission. Additionally, Fig. 4 shows that if γ_p is lower than 15dB, the received signal to interference noise ratio (SINR) at destination of DC is $\frac{\alpha\eta\gamma_P|h_{sd}|^2|h_{sd}|^2}{\gamma_P\sigma_{J1}^2+1}$, which shows an increasing γ_p will lead to an enhancement in OP performance. However, if γ_p increases to a certain degree, the SINR tends to $\frac{\alpha\eta|h_{sd}|^2|h_{sd}|^2}{\sigma_{J1}^2}$, thereby causing the OP arrive at performance floor. The same analysis can be carried out for IP. And the effect of γ_p on NEARS and EARS in terms of OP and IP can be analyzed as DC scheme. Moreover, the IP of EARS is the same as NEARS. This can be explained that the CSIs of wiretap channels from CRs to Es is unavailable for CRs in NEARS and our proposed EARS schemes. Consequently, the IP performance for both two relay selection schemes achieves no benefits with an increasing number of CRs.

In Fig. 5, we depict OPs and IPs for DC, NEARS and EARS schemes versus η. It is seen from Fig. 5 that the efficiency of energy conversion η increases from 0 to 1 results in the reduction of OPs for all schemes. While, the IP performance of these three schemes becomes to be deteriorated as η increases.

This article has been accepted for publication in a future issue of this journal, but has not been fully edited. Content may change prior to final publication. Citation information: DOI 10.1109/TVT.2020.2979267, IEEE Transactions on Vehicular Technology

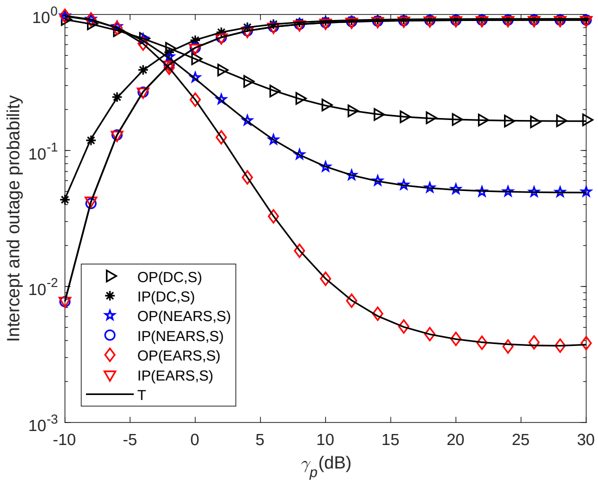

Fig. 4. IPs and OPs of DC and NEARS as well as EARS schemes versus γ_p with $\alpha = 0.4$, $\eta = 0.6$, $\theta = 0.8$, $\gamma_I = 20$dB, $\sigma_{sd}^2 = \sigma_{si}^2 = \sigma_{id}^2 = 0.5$, $\sigma_{ps}^2 = \sigma_{pi}^2 = 0.2$, $\sigma_{ip}^2 = \sigma_{sp}^2 = 0.2$, $\sigma_{J1}^2 = \sigma_{J2}^2 = \sigma_{Ji}^2 = 0.2$, MER=10dB, $T = 1$s, $N_r = 5$, $N_v = 8$.

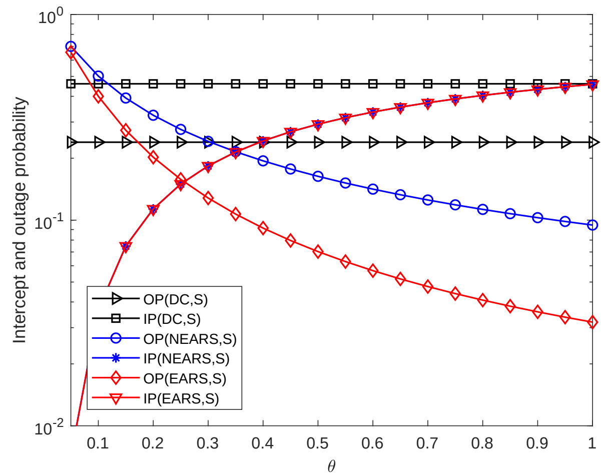

Fig. 6. SRT of DC and NEARS as well as EARS schemes versus θ with $\alpha = 0.4$, $\eta = 0.8$, $\gamma_I = 20$dB, $\sigma_{sd}^2 = \sigma_{si}^2 = \sigma_{id}^2 = 0.5$, $\sigma_{ps}^2 = \sigma_{pi}^2 = 0.4$, $\sigma_{ip}^2 = \sigma_{sp}^2 = 0.2$, $\sigma_{se}^2 = \sigma_{ie}^2 = 0.1$, $\sigma_{J1}^2 = \sigma_{J2}^2 = \sigma_{Ji}^2 = 0.4$, $T = 1$s, $N_r = 4$, $N_v = 1$ and γ_p=5dB.

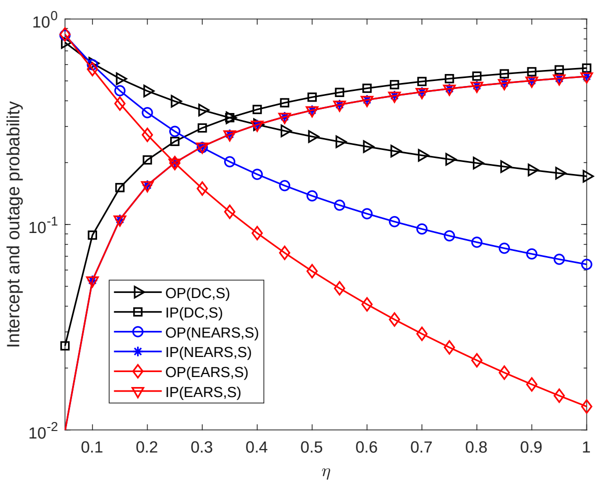

Fig. 5. SRT of DC and NEARS as well as EARS schemes versus η with $\alpha = 0.4$, $\theta = 0.8$, $\gamma_I = 20$dB, $\sigma_{sd}^2 = \sigma_{si}^2 = \sigma_{id}^2 = 0.5$, $\sigma_{ps}^2 = \sigma_{pi}^2 = 0.4$, $\sigma_{ip}^2 = \sigma_{sp}^2 = 0.2$, $\sigma_{se}^2 = \sigma_{ie}^2 = 0.1$, $\sigma_{J1}^2 = \sigma_{J2}^2 = \sigma_{Ji}^2 = 0.4$, $T = 1$s, $N_r = 4$, $N_v = 1$ and γ_p=5dB.

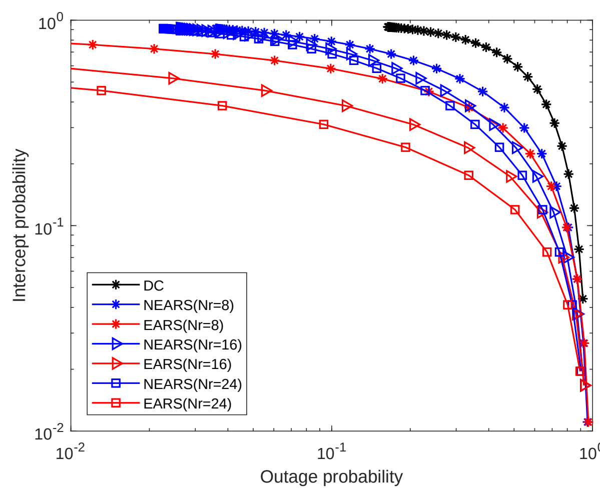

Fig. 7. SRT of DC and NEARS as well as EARS schemes for different N_r with $\alpha = 0.4$, $\eta = 0.6$, $\theta = 0.8$, $\gamma_I = 20$dB, $\sigma_{sd}^2 = \sigma_{si}^2 = \sigma_{id}^2 = 0.5$, $\sigma_{ps}^2 = \sigma_{pi}^2 = 0.2$, $\sigma_{ip}^2 = \sigma_{sp}^2 = 0.2$, $\sigma_{J1}^2 = \sigma_{J2}^2 = \sigma_{Ji}^2 = 0.2$, $T = 1$s, $N_v = 8$, MER=10dB and γ_p=[-10,30]dB.

This phenomenon can be explained that more harvested energy will be used for cognitive transmission with an increasing η, enhancing the received SINR at CD and Es, separately. Additionally, Fig. 6 shows that OPs and IPs versus remaining ratio θ of total energy harvested from PT at each CR for transmitting information. One can clearly see from Fig. 6 that the OP performance of EARS and NEARS is worse than that of DC when a large number of energy at selected CR are used to decode, demodulate, re-code and re-modulate. While with an increasing θ, the more energy is employed to transmit information, which significantly enhances OP performance for EARS and NEARS and leads to EARS and NEARS achieve better performance than DC in terms of OP.

Fig. 7 shows that the SRT of DC, NEARS and EARS schemes versus different N_r. It is clear to see that our proposed EARS scheme performs better than DC and NEARS in terms of SRT performance. Moreover, the number of CRs increases from 8 to 24 causes the SRT performance of EARS and NEARS improve, apparently. This evidently illustrates that SRT performance benefits from multiple relays in cognitive transmission. In addition, the SRT performance gap of EARS is more notable than that of NEARS as the number of CRs increases from 8 to 24, which also further indicates that the superiority of our proposed EARS scheme in terms of SRT. Fig. 8 shows that the SRT performance of these three schemes becomes deteriorated as N_v increases from 1 to 4. As a result, the more private information of cognitive radio systems leaks to Es.

Fig. 9 shows that the SRT of DC and NEARS as well as EARS schemes versus different MER ($\sigma_{id}^2/\sigma_{ie}^2$) which is

This article has been accepted for publication in a future issue of this journal, but has not been fully edited. Content may change prior to final publication. Citation information: DOI 10.1109/TVT.2020.2979267, IEEE Transactions on Vehicular Technology

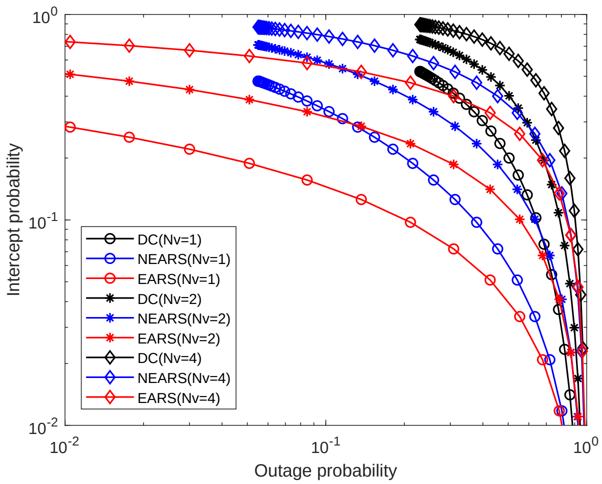

Fig. 8. SRT of DC and NEARS as well as EARS schemes for different N_v with $\alpha = 0.3$, $\eta = 0.8$, $\theta = 0.8$, $\gamma_I = 20$dB, $\sigma_{sd}^2 = \sigma_{si}^2 = \sigma_{id}^2 = 0.5$, $\sigma_{ps}^2 = \sigma_{pi}^2 = 0.2$, $\sigma_{ip}^2 = \sigma_{sp}^2 = 0.2$, $\sigma_{ie}^2 = \sigma_{se}^2 = 0.1$, $\sigma_{J1}^2 = \sigma_{J2}^2 = \sigma_{Ji}^2 = 0.2$, $T = 1$s, $N_r = 10$ and γ_p=[-10,30]dB.

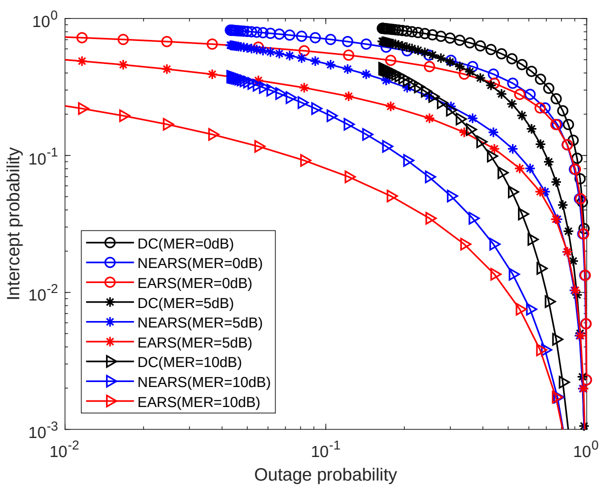

Fig. 9. SRT of DC, NEARS and EARS schemes for different MER with $\alpha = 0.4$, $\eta = 0.6$, $\theta = 0.8$, $\gamma_I = 20$dB, $\sigma_{sd}^2 = \sigma_{si}^2 = \sigma_{id}^2 = 0.5$, $\sigma_{ps}^2 = \sigma_{pi}^2 = 0.1$, $\sigma_{ip}^2 = \sigma_{sp}^2 = 0.1$, $\sigma_{J1}^2 = \sigma_{J2}^2 = \sigma_{Ji}^2 = 0.1$, $T = 1$s, $N_r = 6$, $N_v = 1$ and γ_p=[-10,30]dB.

main-to-eavesdropper ratio [8], [14] and [17]. It is shown from Fig. 9 that MER increases from 0dB to 10dB causes the SRT performance of these three schemes improve, accordingly. To be more specific, if an IP is given by a specific value, the OPs of these three schemes significantly reduces as MER increases. In other words, the security can be achieved at the cost of reliability for cognitive wireless transmission. From Fig. 10, we can see that the similar SRT performance of DC, NEARS and EARS in SISO can be got in MIMO. Moreover, the SRT performance of MIMO performs better than that of SISO and the increasing antenna numbers at CS, CR and CD will significantly enhance the SRT performance for cognitive transmission.

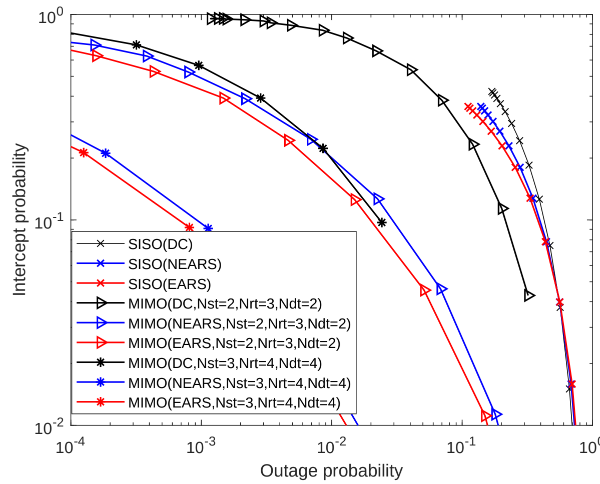

Fig. 10. SRT of DC, NEARS and EARS schemes for different MER with $\alpha = 0.4$, $\eta = 0.6$, $\theta = 0.8$, $\gamma_I = 20$dB, $\sigma_{sd}^2 = \sigma_{si}^2 = \sigma_{id}^2 = 0.5$, $\sigma_{ps}^2 = \sigma_{pi}^2 = 0.2$, $\sigma_{ip}^2 = \sigma_{sp}^2 = 0.2$, $\sigma_{J1}^2 = \sigma_{J2}^2 = \sigma_{Ji}^2 = 0.2$, $T = 1$s, $N_r = 2$, $N_v = 1$, $N_{et} = 2$, MER=10dB and γ_p=[-10,20]dB.

V. Conclusion

We have studied the physical layer security in terms of SRT performance for a CCR-EH system, where a CS having energy harvester communicates with a CD assisted by multiple CRs who are equipped with energy harvesters. Meanwhile, multiple Es were assumed to tap the confidential CS-CD transmission resulted from the broadcast nature of wireless communications. To fight against eavesdropping attacks, we proposed NEARS and EARS schemes depending on whether the CSIs of energy links spanning from PT to CRs are unknown or known to CRs. Additionally, we compared the SRT performance of EARS with that of DC and NEARS schemes. Closed-form expressions of OP and IP for all aforementioned three schemes were derived. Numerical results showed that our proposed EARS scheme has obvious advantages over DC and NEARS in terms of SRT.

Appendix A
Derivations of (28) and (29)

Let denote $X_1 = |h_{ps}|^2$ and $Y_1 = |h_{sp}|^2$, and consider that they are independently and exponentially distributed with respective means σ_{ps}^2 and σ_{sp}^2. Thus, the PDFs of X_1 and Y_1 are separately expressed as

$$f_{X_1}(x_1) = \frac{1}{\sigma_{ps}^2} \exp\left(-\frac{x_1}{\sigma_{ps}^2}\right) \tag{A.1}$$

and

$$f_{Y_1}(y_1) = \frac{1}{\sigma_{sp}^2} \exp\left(-\frac{y_1}{\sigma_{sp}^2}\right). \tag{A.2}$$

Then according to (A.1) and (A.2), we can respectively compute (26) and (27) as

$$\begin{aligned} P_{\text{out,I}}^{\text{dc}} = \int_0^\infty & [1-\exp(-\tfrac{\lambda_0}{a\gamma_{p1}\sigma_{sd}^2 x_1})] \\ & \times [1-\exp(-\tfrac{\gamma_{I1}}{a\gamma_{p1}\sigma_{sp}^2 x_1})] f_{X_1}(x_1)dx_1 \end{aligned} \tag{A.3}$$

and

$$P_{\text{out,II}}^{\text{dc}} = \int_0^\infty [1-\exp(-\frac{\lambda_0}{\gamma_{I1}\sigma_{sd}^2}y_1)] \times \exp(-\frac{\gamma_{I1}}{a\gamma_{p1}\sigma_{ps}^2 y_1}) f_{Y_1}(y_1)dy_1 , \quad (A.4)$$

which can be further respectively given by

$$P_{\text{out,I}}^{\text{dc}} = 1 - \sqrt{\frac{\varepsilon_1\gamma_{I1}}{\sigma_{sp}^2}}K_1(\sqrt{\frac{\varepsilon_1\gamma_{I1}}{\sigma_{sp}^2}}) - \sqrt{\frac{\varepsilon_1\lambda_0}{\sigma_{sd}^2}} \times K_1(\sqrt{\frac{\varepsilon_1\lambda_0}{\sigma_{sd}^2}}) + \sqrt{\varepsilon_1\varepsilon_2}K_1(\sqrt{\varepsilon_1\varepsilon_2}) \quad (A.5)$$

and

$$P_{\text{out,II}}^{\text{dc}} = \sqrt{\frac{\varepsilon_1\gamma_{I1}}{\sigma_{sp}^2}}K_1(\sqrt{\frac{\varepsilon_1\gamma_{I1}}{\sigma_{sp}^2}}) - \frac{\gamma_{I1}}{\sigma_{sp}^2}\sqrt{\frac{\varepsilon_1}{\varepsilon_2}}K_1(\sqrt{\varepsilon_1\varepsilon_2}), \quad (A.6)$$

where $\varepsilon_1 = \frac{4}{a\gamma_{p1}\sigma_{ps}^2}$ and $\varepsilon_2 = \frac{\lambda_0}{\sigma_{sd}^2} + \frac{\gamma_{I1}}{\sigma_{sp}^2}$. Then substituting (A.5) and (A.6) into (25), the closed-form expression of $P_{\text{out}}^{\text{dc}}$ can be easily formulated.

Appendix B
Derivations of (35) and (36)

Depending on the PDF of X_1 and Y_1, we can rewrite (33) and (34) as

$$\begin{aligned} P_{\text{int,I}}^{\text{dc}} &= \int_0^\infty \Pr(\sum_{e=1}^{N_v}|h_{se}|^2 > \frac{\lambda_s}{a\gamma_{p2}x_1}) \times \Pr(|h_{sp}|^2 < \frac{\gamma_{I2}}{a\gamma_{p2}x_1}) f_{X_1}(x_1)dx_1 \\ &= \int_0^\infty [1 - F_{\sum_{e=1}^{N_v}|h_{se}|^2}(\frac{\lambda_s}{a\gamma_{p2}x_1})] \times F_{|h_{sp}|^2}(\frac{\gamma_{I2}}{a\gamma_{p2}x_1}) f_{X_1}(x_1)dx_1 \end{aligned} \quad (B.1)$$

and

$$\begin{aligned} P_{\text{int,II}}^{\text{dc}} &= \int_0^\infty \Pr(\sum_{e=1}^{N_v}|h_{se}|^2 > \frac{\lambda_s}{\gamma_{I2}}y_1) \times \Pr(|h_{ps}|^2 > \frac{\gamma_{I2}}{b\gamma_{p2}y_1}) f_{Y_1}(y_1)dy_1 \\ &= \int_0^\infty [1 - F_{\sum_{e=1}^{N_v}|h_{se}|^2}(\frac{\lambda_s}{\gamma_{I2}}y_1)] \times [1 - F_{|h_{ps}|^2}(\frac{\gamma_{I2}}{b\gamma_{p2}y_1})] f_{Y_1}(y_1)dy_1 \end{aligned} . \quad (B.2)$$

According to [25], we have the CDF of $\sum_{e=1}^{N_v}|h_{se}|^2$

$$F_{\sum_{e=1}^{N_v}|h_{se}|^2}(z) = 1 - \exp(-\frac{z}{\sigma_{se}^2})\sum_{g=0}^{N_v-1}\frac{z^g}{g!\sigma_{se}^{2g}}. \quad (B.3)$$

Substituting (B.3) into (B.1) and (B.2), we can respectively get $P_{\text{int,I}}^{\text{dc}}$ and $P_{\text{int,II}}^{\text{dc}}$ as (B.4) and (B.5), where $\Lambda_1 = \frac{\lambda_s}{a\gamma_{p2}\sigma_{se}^2}$, $\Lambda_2 = \frac{\gamma_{I2}}{a\gamma_{p2}\sigma_{sp}^2}$, $\Lambda_3 = \frac{\lambda_s}{\gamma_{I2}\sigma_{se}^2}$ and $\Lambda_4 = \frac{\gamma_{I2}}{a\gamma_{p2}\sigma_{ps}^2}$

Thus, combining (B.4) and (B.5) as well as (32), we can obtain the closed-form expression of $P_{\text{int}}^{\text{dc}}$.

Appendix C
Derivations of (47) and (48)

We consider that $|h_{pi}|^2$, $|h_{id}|^2$ and $|h_{ip}|^2$ are independently and exponential distributed random variables with respective means σ_{pi}^2, σ_{id}^2 and σ_{ip}^2. For notational simplicity, denoting $X_2 = |h_{pi}|^2$, $Y_2 = |h_{id}|^2$ and $Z_2 = |h_{ip}|^2$. Hence, the joint PDF of (X_2, Y_2) and (Y_2, Z_2) can be expressed as

$$f_{X_2,Y_2}(x_2,y_2) = \frac{1}{\sigma_{pi}^2\sigma_{id}^2}\exp(-\frac{x_2}{\sigma_{pi}^2} - \frac{y_2}{\sigma_{id}^2}) \quad (C.1)$$

and

$$f_{Y_2,Z_2}(y_2,z_2) = \frac{1}{\sigma_{id}^2\sigma_{ip}^2}\exp(-\frac{y_2}{\sigma_{id}^2} - \frac{z_2}{\sigma_{ip}^2}). \quad (C.2)$$

Therefore, substituting (C.1) and (C.2) into (45) and (46), separately, yields

$$P_{\text{out,I\_1}}^{\text{NEARS}} = \iint_\Phi \Pr(|h_{ip}|^2 < \frac{\gamma_{I1}}{b\gamma_{p1}x_2}) \times \prod_{k\in D_n, k\neq i}\Pr(|h_{kd}|^2 < y_2) f_{X_2,Y_2}(x_2,y_2)dx_2dy_2 \quad (C.3)$$

and

$$P_{\text{out,I\_2}}^{\text{NEARS}} = \iint_\tau \Pr(|h_{pi}|^2 > \frac{\gamma_{I1}}{b\gamma_{p1}z_2}) \times \prod_{k\in D_n, k\neq i}\Pr(|h_{kd}|^2 < y_2) f_{Y_2,Z_2}(y_2,z_2)dy_2dz_2 , \quad (C.4)$$

where $\Phi = \{(x_2,y_2)|b\gamma_{p1}x_2y_2 < \lambda_1, x_2 > 0, y_2 > 0\}$ and $\tau = \{(y_2,z_2)|\gamma_{I1}y_2 < \lambda_1 z_2,\ y_2 > 0,\ z_2 > 0\}$. In addition, D_n represents the n-th non-subset of CRs. Moreover, $\prod_{k\in D_n, k\neq i}\Pr(|h_{kd}|^2 < y_2)$ can be further got with the aid of binomial theorem, yielding

$$\prod_{k\in D_n, k\neq i}\Pr(|h_{kd}|^2 < y_2) = 1 + \sum_{m=1}^{2^{|D_n(m)|-1}-1}(-1)^{|D_n(m)|}\exp(-\sum_{k\in D_n(m)}\frac{y_2}{\sigma_{kd}^2}) . \quad (C.5)$$

Then combining (C.5) and (C.3), we obtain

$$P_{\text{out,I\_1}}^{\text{NEARS}} = \psi_{\text{III\_1}} + \psi_{\text{III\_2}} - \psi_{\text{III\_3}} - \psi_{\text{III\_4}}, \quad (C.6)$$

where $\psi_{\text{III\_1}}$, $\psi_{\text{III\_2}}$, $\psi_{\text{III\_3}}$ and $\psi_{\text{III\_4}}$ are formulated as

$$\psi_{\text{III\_1}} = \iint_\Phi f_{X_2,Y_2}(x_2,y_2)dx_2dy_2, \quad (C.7)$$

$$\psi_{\text{III\_2}} = \sum_{m=1}^{2^{|D_n|-1}-1}(-1)^{|D_n(m)|}\iint_\Phi \exp(-\sum_{k\in D_n(m)}\frac{y_2}{\sigma_{kd}^2}) , \times f_{X_2,Y_2}(x_2,y_2)dx_2dy_2 \quad (C.8)$$

$$\psi_{\text{III\_3}} = \iint_\Phi \exp(-\frac{\gamma_{I1}}{b\gamma_{p1}\sigma_{ip}^2x_2}) f_{X_2,Y_2}(x_2,y_2)dx_2dy_2 \quad (C.9)$$

This article has been accepted for publication in a future issue of this journal, but has not been fully edited. Content may change prior to final publication. Citation information: DOI 10.1109/TVT.2020.2979267, IEEE Transactions on Vehicular Technology

$$
\begin{aligned}
P_{\text{int,I}}^{\text{dc}} &= \int_0^\infty \exp(-\frac{\lambda_s}{a\gamma_{p2}\sigma_{se}^2 x_1}) \sum_{g=0}^{N_e-1} \frac{\lambda_s^g x_1^{-g}}{g!(a\gamma_{p2}\sigma_{se}^2)^g} \ (1-\exp(-\frac{\gamma_{I2}}{a\gamma_{p2}\sigma_{sp}^2 x_1}))f_{X_1}(x_1)dx_1 \\
&= \sum_{g=0}^{N_e-1} \frac{2{\Lambda_1}^g}{g!\sigma_{ps}^2}(\Lambda_1\sigma_{ps}^2)^{\frac{1-g}{2}} K_{1-g}(2\sqrt{\Lambda_1\sigma_{ps}^{-2}}) - \sum_{g=0}^{N_e-1} \frac{2{\Lambda_1}^g}{g!\sigma_{ps}^2}[(\Lambda_1+\Lambda_2)\sigma_{ps}^2]^{\frac{1-g}{2}} K_{1-g}(2\sqrt{(\Lambda_1+\Lambda_2)\sigma_{ps}^{-2}})
\end{aligned} . \tag{B.4}
$$

$$
\begin{aligned}
P_{\text{int,II}}^{\text{dc}} &= \int_0^\infty \exp(-\frac{\lambda_s y_1}{\gamma_{I2}\sigma_{se}^2}) \sum_{g=0}^{N_e-1} \frac{\lambda_s^g y_1^g}{g!(\gamma_{I2}\sigma_{se}^2)^g} \exp(-\frac{\gamma_{I2}}{a\gamma_{p2}\sigma_{ps}^2 y_1})f_{Y_1}(y_1)dy_1 \\
&= \sum_{g=0}^{N_e-1} \frac{2{\Lambda_3}^g}{g!\sigma_{sp}^2}[\Lambda_4(\Lambda_3+\sigma_{sp}^{-2})^{-1}]^{\frac{g+1}{2}} K_{1+g}(2\sqrt{\Lambda_4(\Lambda_3+\sigma_{sp}^{-2})})
\end{aligned} . \tag{B.5}
$$

and

$$
\begin{aligned}
\psi_{\text{III\_4}} = & \sum_{m=1}^{2^{|D_n|-1}-1} (-1)^{|D_n(m)|} \iint_{\Phi} \exp(-\frac{\gamma_{I1}}{b\gamma_{p1}\sigma_{ip}^2 x_2}) \\
& \times \exp(-\sum_{k\in D_n(m)} \frac{y_2}{\sigma_{kd}^2}) f_{X_2,Y_2}(x_2,y_2)dx_2dy_2
\end{aligned} . \tag{C.10}
$$

Combining (C.1) and (C.7), we have

$$
\psi_{\text{III\_1}} = 1-\sqrt{\Lambda_5\lambda_1}K_1(\sqrt{\Lambda_5\lambda_1}), \tag{C.11}
$$

where $\Lambda_5 = \frac{4}{b\gamma_{p1}\sigma_{id}^2\sigma_{pi}^2}$. Similarly, with the aid of $f_{X_2,Y_2}(x_2,y_2)$, (C.8) can be further computed as

$$
\begin{aligned}
& \psi_{\text{III\_2}} \\
&= \sum_{m=1}^{2^{|D_n|-1}-1} \frac{(-1)^{|D_n(m)|}\Lambda_6}{\sigma_{id}^2} - \sum_{m=1}^{2^{|D_n|-1}-1} \frac{(-1)^{|D_n(m)|}\Lambda_6}{\sigma_{id}^2} , \\
& \times \sqrt{\frac{4\lambda_1}{b\gamma_{p1}\Lambda_6\sigma_{pi}^2}} K_1(\sqrt{\frac{4\lambda_1}{b\gamma_{p1}\Lambda_6\sigma_{pi}^2}})
\end{aligned} \tag{C.12}
$$

where $\Lambda_6 = (\frac{1}{\sigma_{id}^2} + \sum_{k\in D_n(m)} \frac{1}{\sigma_{kd}^2})^{-1}$. Besides, $\psi_{\text{III\_3}}$ can also be formulated as

$$
\begin{aligned}
& \psi_{\text{III\_3}} \\
&= \sqrt{\tfrac{\gamma_{I1}\Lambda_7}{\sigma_{ip}^2}} k_1(\sqrt{\tfrac{\gamma_{I1}\Lambda_7}{\sigma_{ip}^2}}) - \sqrt{\Lambda_7(\tfrac{\gamma_{I1}}{\sigma_{ip}^2}+\tfrac{\lambda_1}{\sigma_{id}^2})} K_1(\sqrt{\Lambda_7(\tfrac{\gamma_{I1}}{\sigma_{ip}^2}+\tfrac{\lambda_1}{\sigma_{id}^2})})
\end{aligned} , \tag{C.13}
$$

where $\Lambda_7 = \frac{4}{b\gamma_{p1}\sigma_{pi}^2}$. Moreover, (C.10) can be rewritten as (C.14)

$$
\begin{aligned}
\psi_{\text{III\_4}} = & \sum_{m=1}^{2^{|D_n|-1}-1} \frac{(-1)^{|D_n(m)|}\Lambda_6}{\sigma_{id}^2} \sqrt{\gamma_{I1}\Lambda_5} K_1(\sqrt{\gamma_{I1}\Lambda_5}) \\
& - \sum_{m=1}^{2^{|D_n|-1}-1} \frac{(-1)^{|D_n(m)|}\Lambda_6}{\sigma_{id}^2} \sqrt{\Lambda_8} K_1(\sqrt{\Lambda_8})]
\end{aligned} , \tag{C.14}
$$

wherein, $\Lambda_8 = \frac{\sigma_{id}^2\gamma_{I1}\Lambda_5}{\sigma_{ip}^2} + \frac{4\lambda_1}{b\gamma_{p1}\sigma_{pi}^2\Lambda_6}$. Finally, substituting (C.11), (C.12), (C.13) and (C.14) into (C.6), $P_{\text{out,I\_1}}^{\text{NEARS}}$ can be expressed as (47).

Similarly to (C.3), we can reformulate (C.4) as

$$
P_{\text{out,I\_2}}^{\text{NEARS}} = \psi_{\text{III\_5}} + \psi_{\text{III\_6}}, \tag{C.15}
$$

where $\psi_{\text{III\_5}}$ and $\psi_{\text{III\_6}}$ are given by

$$
\psi_{\text{III\_5}} = \iint_{\tau} \exp(-\frac{\gamma_{I1}}{a\gamma_{p1}\sigma_{pi}^2 z_2}) f_{Y_2,Z_2}(y_2,z_2)dy_2dz_2 \tag{C.16}
$$

and

$$
\begin{aligned}
\psi_{\text{III\_6}} = & \sum_{m=1}^{2^{|D_n|-1}-1} (-1)^{D_n(m)} \iint_{\tau} \exp(-\frac{\gamma_{I1}}{a\gamma_{p1}\sigma_{pi}^2 z_2}) \\
& \times \exp(-\sum_{k\in D_n(m)} \frac{y_2}{\sigma_{kd}^2}) f_{Y_2,Z_2}(y_2,z_2)dy_2dz_2
\end{aligned} . \tag{C.17}
$$

Then, by using the result of (C.2), (C.16) and (C.17) can be respectively rewritten as

$$
\psi_{\text{III\_5}} = \sqrt{\frac{\gamma_{I1}\Lambda_7}{\sigma_{ip}^2}} K_1(\sqrt{\frac{\gamma_{I1}\Lambda_7}{\sigma_{ip}^2}}) - \frac{1}{\sigma_{ip}^2}\sqrt{\frac{\gamma_{I1}\Lambda_7}{\Lambda_9}} K_1(\sqrt{\gamma_{I1}\Lambda_9\Lambda_7}) \tag{C.18}
$$

and

$$
\begin{aligned}
\psi_{\text{III\_6}} = & \sum_{m=1}^{2^{|D_n|-1}-1} \frac{(-1)^{|D_n(m)|}\Lambda_6}{\sigma_{id}^2} \sqrt{\frac{\gamma_{I1}\Lambda_7}{\sigma_{ip}^2}} K_1(\sqrt{\frac{\gamma_{I1}\Lambda_7}{\sigma_{ip}^2}}) \\
& - \sum_{m=1}^{2^{|D_n|-1}-1} \frac{(-1)^{|D_n(m)|}\Lambda_6}{\sigma_{ip}^2\sigma_{id}^2} \sqrt{\gamma_{I1}\Lambda_7(\frac{1}{\sigma_{ip}^2}+\frac{\lambda_1}{\gamma_{I1}\Lambda_6})}, \\
& \times K_1(\sqrt{\gamma_{I1}\Lambda_7(\frac{1}{\sigma_{ip}^2}+\frac{\lambda_1}{\gamma_{I1}\Lambda_6})})
\end{aligned} \tag{C.19}
$$

where $\Lambda_9 = \frac{1}{\sigma_{ip}^2} + \frac{\lambda_1}{\gamma_{I1}\sigma_{id}^2}$. Hence, the final expression of $P_{\text{out,I\_2}}^{\text{NEARS}}$ can be got as (48) using the results of (C.18) and (C.19), which completes the proof of (47) and (48).

References

[1] Y. Wu, A. Khisti, C. Xiao, G. Caire, K. Wong, and X. Gao, "A survey of physical layer security techniques for 5G wireless networks and challenges ahead," *IEEE J. Sel. Areas Commun.*, vol. 36, no. 4, pp. 679-695, Apr. 2018.

[2] H. Yu, S. Guo, Y. Yang, L. Ji, and Y. Yang, "Secrecy energy efficiency optimization for Ddownlink two-user OFDMA networks with SWIPT," *IEEE Systems Journal.*, vol. 13, no. 1, pp. 324-335, Mar. 2019.

[3] X. Tang, Y. Cai, Y. Deng, Y. Huang, W. Yang, and W. Yang, "Energy-constrained SWIPT networks: enhancing physical layer security with FD self-jamming," *IEEE Trans.Inf. Forensics Security*, vol. 14, no. 1, pp. 212-222, Jan. 2019.

[4] J. Men, J. Ge, and C. Zhang, "A joint relay-and-antenna selection scheme in energy-harvesting MIMO relay networks," *IEEE Signal Processing Lett.*, vol. 23, no. 4, pp. 532-536, Apr. 2016.

This article has been accepted for publication in a future issue of this journal, but has not been fully edited. Content may change prior to final publication. Citation information: DOI 10.1109/TVT.2020.2979267, IEEE Transactions on Vehicular Technology

[5] A. A. Nasir, X. Zhou, S. Durrani, and R. A. Kennedy, " Relaying protocols for wireless energy harvesting and information processing," *IEEE Trans. Wireless Commun.*, vol. 12, no. 7, pp. 3622-3636, July 2013.

[6] S. K. Yadav and T. Acharaya, "Outage analysis in cooperative cognitive radio networks with simultaneous wireless information and power transfer," in *Proc. IEEE Conf. Commun. (SPCOM)*, Bangalore, 2016, pp. 1-5.

[7] D. Wang, R. Zhang, X. Cheng, and L. Yang, "Capacity-enhancing full-duplex relay networks based on power-splitting (PS-)SWIPT," *IEEE Trans. Veh. Technol.*, vol. 66, no. 6, pp. 5445-5450, June 2017.

[8] Y. Zou, X. Wang, and W. Shen, "Optimal relay selection for physical-layer security in cooperative wireless networks," *IEEE J. Sel. Areas Commun.*, vol. 31, no. 10, pp. 2099-2111, Oct. 2013.

[9] D. Wang, B. Bai, W. Zhao, and Z. Han, "A survey of optimization Aapproaches for wireless physical layer security," *IEEE Commun. Surv. Tut.*, vol. 21, no. 2, pp. 1878-1911, Secondquarter 2019.

[10] A. D. Wyner, "The wire-tap channel," *Bell Syst. Tech. J.*, vol. 54, no. 8, pp. 1355-1387, 1975.

[11] H. Guo, Z. Yang, L. Zhang, J. Zhu, and Y. Zou, "Power-constrained secrecy rate maximization for joint relay and jammer selection assisted wireless networks," *IEEE Trans. Commun.*, vol. 65, no. 5, pp. 2180-2193, May 2017.

[12] H. Lei ,*et al.*, "Secrecy outage analysis for cooperative NOMA systems with relay selection scheme," *IEEE Trans. Commun.*, vol. 67, no. 9, pp. 6282-6298, Sept. 2019.

[13] H. Lei ,*et al.*, "On secrecy outage of relay selection in underlay cognitive radio networks over Nakagami-m fading channel," *IEEE Trans. Cogn. Commun. Netw.*, vol. 3, no. 4, pp. 614-627, Dec. 2017.

[14] J. Zhu, Y. Zou, G. Wang, Y. Yao, and G. K. Karagiannidis, "On secrecy performance of antenna-selection-aided MIMO systems against eavesdropping," *IEEE Trans. Veh. Technol.*, vol. 65, no. 1, pp. 214-225, Jan. 2016.

[15] H. Lei ,*et al.*, "Secrecy outage performance of transmit antenna selection for MIMO underlay cognitive radio systems over nakagami-m channels," *IEEE Trans. Veh. Technol.*, vol. 66, no. 3, pp. 2237-2250, Mar. 2017.

[16] S. Asaad, A. Bereyhi, A. M. Rabiei, R. R. Mller, and R. F. Schaefer, "Optimal transmit antenna selection for massive MIMO wiretap channels," *IEEE J. Sel. Areas Commun.*, vol. 66, no. 9, pp. 1518-1531, Sept. 2017.

[17] Y. Zou, X. Wang, and W. Shen, "Physical-layer security with multiuser scheduling in cognitive radio networks," *IEEE Trans. Commun.*, vol. 61, no. 12, pp. 5103-5113, Dec. 2013.

[18] B. Li, Y. Zou, J. Zhou, F. Wang, W. Cao, and Y. Yao, "Secrecy outage probability analysis of friendly jammer selection aided multiuser scheduling for wireless networks," *IEEE Trans. Commun.*, vol. 67, no. 5, pp. 3482-3495, May 2019.

[19] H. Xing, L. Liu, and R. Zhang, "Secrecy wireless information and power transfer in fading wiretap channel," *IEEE Trans. Veh. Technol.*, vol. 65, no. 1, pp. 180-190, Jan. 2016.

[20] X. Liu, Z. Li, and C. Wang, "Secure decode-and-forward relay SWIPT systems with power splitting schemes," *IEEE Trans. Veh. Technol.*, vol. 67, no. 8, pp. 7341-7354, Aug. 2018.

[21] S. S. Kalamkar and A. Banerjee, "Secure communication via a wireless energy harvesting untrusted relay," *IEEE Trans. Veh. Technol.*, vol. 66, no. 3, pp. 2199-2213, Mar. 2017.

[22] T. M. Hoang, T. Q. Duong, N. Vo, and C. Kundu, *et al.*, "Physical layer security in cooperative energy harvesting networks with a friendly jammer," *IEEE Wireless Commun, Lett.*, vol. 6, no. 2, pp. 174-177, Apr. 2017.

[23] V. Nhan Vo, T. G. Nguyen, C. So-In, Z. A. Baig, and S. Sanguanpong, "Secrecy outage performance analysis for energy harvesting sensor networks with a jammer using relay selection strategy," *IEEE Access*, vol. 6, pp. 23406-23419, 2018.

[24] H. Lei, Z. Dai, K. Park, W. Lei, G. Pan and M. Alouini, "Secrecy outage analysis of mixed RF-FSO downlink SWIPT systems," *IEEE Trans. Commun.*, vol. 66, no. 12, pp. 6384-6395, Dec. 2018.

[25] N. Zhao, F. R. Yu, and V. C. M. Leung, "Wireless energy harvesting in interference alignment networks," *IEEE Commun. Maga.*, vol. 53, no. 6, pp. 72-78, Jun. 2015.

[26] N. Zhao, Y. Cao, F. R. Yu, Y. Chen, M. Jin, and V. C. M. Leung, "Artificial noise assisted secure interference networks with wireless power transfer," *IEEE Trans. Veh. Technol.*, vol. 67, no. 2, pp. 1087-1098, Feb. 2018.

[27] N. Zhao, S. Zhang, F. R. Yu, Y. Chen, A. Nallanathan, and V. C. M. Leung, "Exploiting interference for energy harvesting: a survey, research issues, and challenges," *IEEE Access*, vol. 5, pp. 10403-10421, 2017.

[28] H. Lei, M. Xu, I. S. Ansari, G. Pan, K. A. Qaraqe, and M. Alouini, "On secure underlay MIMO cognitive radio networks with energy harvesting and transmit antenna selection," *IEEE Trans. Green Commun. and Netw.*, vol. 1, no. 2, pp. 192-203, June 2017.

[29] X. Ding, Y. Zou, G. Zhang, X. Chen, X. Wang, and L. Hanzo, "The security-reliability tradeoff of multiuser scheduling aided energy harvesting cognitive radio networks," *IEEE Trans. Commun.*, vol. 67, no. 6, pp. 3890-3904, June 2019.

[30] M. Li, H. Yin, Y. Huang, Y. Wang, and R. Yu, "Physical layer security in overlay cognitive radio networks with energy harvesting," *IEEE Trans. Veh. Technol.*, vol. 67, no. 11, pp. 11274-11279, Nov. 2018.

[31] X. Chen, L. Guo, X. Li, C. Dong, J. Lin, and P. T. Mathiopoulos, "Secrecy rate optimization for cooperative cognitive radio networks aided by a wireless energy harvesting jammer," *IEEE Access*, vol. 6, pp. 34127-34134, 2018.

[32] M. Xu, T. Jing, X. Fan, Y. Wen, and Y. Huo, "Secure transmission solutions in energy harvesting enabled cooperative cognitive radio networks," in *Proc. IEEE Conf. Commun. (WCNC)*, Barcelona, 2018, pp. 1-6.

[33] S. Gautam, T. X. Vu, S. Chatzinotas, and B. Ottersten, "Cache-aided simultaneous wireless information and power transfer (SWIPT) with relay selection," *IEEE J. Sel. Areas Commun.*, vol. 37, no. 1, pp. 187-201, Jan. 2019.

[34] P. Yan, Y. Zou, and J. Zhu, "Energy-aware multiuser scheduling for physical-layer security in energy-harvesting underlay cognitive radio systems," *IEEE Trans. Veh. Technol.*, vol. 67, no. 3, pp. 2084-2096, Mar. 2018.

[35] H. Alves, R. D. Souza, M. Debbah, and M. Bennis, "Performance of transmit antenna selection physical layer security schemes," *IEEE Signal Process. Lett.*, vol. 19, no. 6, pp. 372C375, June 2012.

[36] N. Yang, P. L. Yeoh, M. Elkashlan, R. Schober, and I. B. Collings, "Transmit antenna selection for security enhancement in MIMO wiretap channels" *IEEE Trans. Commun.*, vol. 61, no. 1, pp. 144-154, Jan. 2013.

[37] J. N. Laneman, D. N. C. Tse, and G. W. Wornell, "Cooperative diversity in wireless networks: Efficient protocols and outage behavior," *IEEE Trans. Inf. Theory*, vol. 50, no. 12, pp. 3062-3080, Dec. 2004.

[38] X. Chen, L. Lei, H. Zhang, and C. Yuen, "Large-scale MIMO relaying techniques for physical layer security: AF or DF?," *IEEE Trans. Wireless Commun.*, vol. 14, no. 9, pp. 5135-5146, Sept. 2015.

[39] X. Tang, R. Liu, P. Spasojevic, and H. V. Poor, "On the throughput of secure hybrid-ARQ protocols for Gaussian block-fading channels," *IEEE Trans. Inf. Theory*, vol. 55, no. 4, pp. 1575-1591, Apr. 2009.

[40] Y. Zou, "Intelligent interference exploitation for heterogeneous cellular networks against eavesdropping," *IEEE J. Sel. Areas Commun.*, vol. 36, no. 7, pp. 1453-1464, July 2018.

[41] I. S. Gradshteyn and I.M. Ryzhik, "Table of integrals, series, and products," *7th ed. New York, NY, USA: Academic*, 2007.

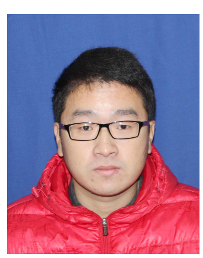

Peishun Yan received the B.Eng. degree in Electronic and Information Engineering from Nantong University (NTU), Nantong, China, in 2015 and the M.S. degree in Signal and Information Processing from Nanjing University of Posts and Telecommunications (NUPT), Nanjing, China, in 2018, where he is currently pursuing the Ph.d. degree. His research interests include cognitive radio, cooperative communications, wireless security and quantum communications.

Yulong Zou (SM'13) is a Full Professor and Doctoral Supervisor at the Nanjing University of Posts and Telecommunications (NUPT), Nanjing, China. He received the B.Eng. degree in information engineering from NUPT, Nanjing, China, in July 2006, the first Ph.D. degree in electrical engineering from the Stevens Institute of Technology, New Jersey, USA, in May 2012, and the second Ph.D. degree in signal and information processing from NUPT, Nanjing, China, in July 2012.

Dr. Zou was awarded the 9th IEEE Communications Society Asia-Pacific Best Young Researcher in 2014 and a co-receipt of the Best Paper Award at the 80th IEEE Vehicular Technology Conference in 2014. He has served as an editor for the IEEE Communications Surveys & Tutorials, IEEE Communications Letters, EURASIP Journal on Advances in Signal Processing, IET Communications, and China Communications. In addition, he has acted as TPC members for various IEEE sponsored conferences, e.g., IEEE ICC/GLOBECOM/WCNC/VTC/ICCC, etc.

Xiaojin Ding received the Ph.D. degree in information and communication engineering from the National Mobile Communication Research Laboratory, Southeast University (SEU), Nanjing, China. He is currently a Lecturer with the Nanjing University of Posts and Telecommunications (NUPT), Nanjing. His research interests include space information networks, cooperative communications, and physical-layer security.

Jia Zhu is a Full Professor at the Nanjing University of Posts and Telecommunications (NUPT), Nanjing, China. She received the B.Eng. degree in Computer Science and Technology from the Hohai University, Nanjing, China, in July 2005, and the Ph.D. degree in Signal and Information Processing from the Nanjing University of Posts and Telecommunications, Nanjing, China, in April 2010. From June 2010 to June 2012, she was a Postdoctoral Research Fellow at the Stevens Institute of Technology, New Jersey, the United States. Since November 2012, she has been a full-time faculty member with the Telecommunication and Information School of NUPT, Nanjing, China. Her general research interests include the cognitive radio, physical-layer security and communications theory.